

UNCLASSIFIED

AD 286 404

*Reproduced
by the*

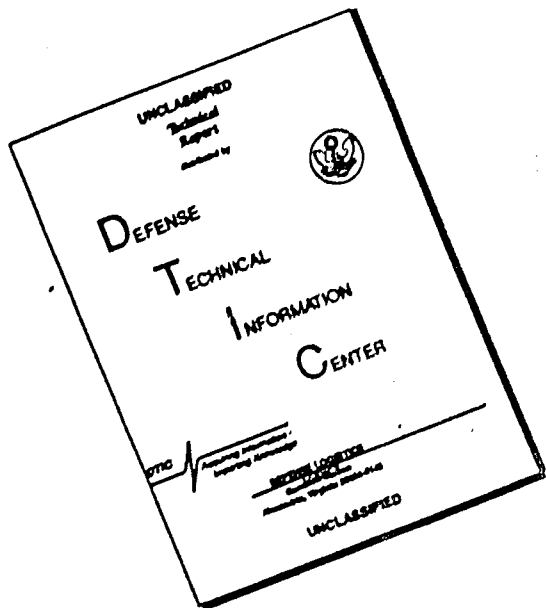
**ARMED SERVICES TECHNICAL INFORMATION AGENCY
ARLINGTON HALL STATION
ARLINGTON 12, VIRGINIA**



UNCLASSIFIED

NOTICE: When government or other drawings, specifications or other data are used for any purpose other than in connection with a definitely related government procurement operation, the U. S. Government thereby incurs no responsibility, nor any obligation whatsoever; and the fact that the Government may have formulated, furnished, or in any way supplied the said drawings, specifications, or other data is not to be regarded by implication or otherwise as in any manner licensing the holder or any other person or corporation, or conveying any rights or permission to manufacture, use or sell any patented invention that may in any way be related thereto.

DISCLAIMER NOTICE



THIS DOCUMENT IS BEST
QUALITY AVAILABLE. THE COPY
FURNISHED TO DTIC CONTAINED
A SIGNIFICANT NUMBER OF
PAGES WHICH DO NOT
REPRODUCE LEGIBLY.

63-1-2

286 404

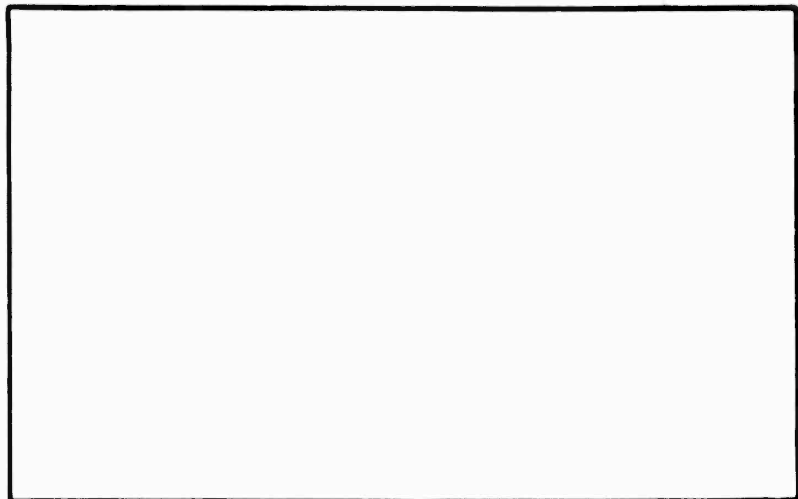
①

286 404



AD No.

ASTIA FILE CARD



SCHOOL OF ENGINEERING

WRIGHT-PATTERSON AIR FORCE BASE, OHIO

AF-WP-O-MAY 62 3,500

#8,10

OCT 24 1962

100-1000

A STUDY OF AN
INDUCTION-COUPLED PLASMA
OPERATING AT 400 KILOCYCLES

Howard R. Cannon

GA/Phys/62-2

A STUDY OF AN
INDUCTION-COUPLED PLASMA
OPERATING AT 400 KILOCYCLES

THESIS

Presented to the Faculty of the School of Engineering of
the Air Force Institute of Technology
Air University
in Partial Fulfillment of the
Requirements for the Degree of
Master of Science

By

Howard R. Cannon, B.S. Mil Sc.

Capt USAF

Graduate Astronautics

August 1962

Preface

This report concerns an elementary investigation of the problems of containing an induction-coupled plasma, measuring the plasma power and temperature, and determining the effects changing plasma operating conditions. I hope this report successfully establishes a starting point for future detailed investigations.

During the period of this study I was the guest of the Aeronautical Research Laboratories, and I wish to thank the members of ARL, who made my visit informative and enjoyable. My thanks particularly to the staff of the Thermomechanics Laboratory, ARL, for their support and encouragement.

I am especially indebted to E. Fender for his guidance and support during his stay in this country, and to W. G. Brown and J. Birkeland, Plasma Physics Laboratory, ARL, for their explanation of Abel's Integral Transformation which appears in Appendix A. My thanks also to my lab partner, A. Shadé, for the time and effort he devoted to assisting me, sometimes at the expense of his own study.

This report could not have been submitted in its present form without the patience and understanding of my Faculty Advisor, R. Wingerson. If time had permitted me to properly act upon his counsel, a far better report would have resulted.

And finally, my thanks to my wife, Carolyn, for her efforts to minimize distractions while I worked.

List of Figures

Figure	Page
1 Plasma-Generator with Clear Water Coolant	55
2 Plasma-Generator with Black Water Coolant	56
3 Experimental apparatus	57
4 Schematic of Plasma-Generator and Calorimeter	58
5 Normalized Relative Intensity as a Function of Temperature	59
6 Normalized Relative Intensity as a Function of Radius . . .	59
7 Typical Observed Intensity of Lambda 7635.2	59
8 Electrical Conductivity as a Function of Temperature . .	59
9 Modified Water Pipe for Mode 3	60
10 Normalized Power, A_2 and A_3 , as a Function of Gas Flow .	61
11 Normalized Power, A_T , as a Function of Gas Flow	62
12 Normalized Power, A_2 , as a Function of Gas Flow	63
13 Normalized Power, A_T , as a Function of Gas Flow	64
14 Wall Loss Ratio as a Function of Gas Flow	65
15 Radiation Ratio as a Function of Gas Flow	66
16 Calorimeter Ratio as a Function of Gas Flow	67
17 Excess Plate Power as a Function of Gas Flow	68
18 Power Coupling as a Function of Channelling Vortex Strength	69
19 Supersonic Heating by Induction-Coupled Plasma	70

List of Tables

Table	Page
I Operating Notes	20
II Sample Power Exposure Data, Node 3	23
III Filtered Node Power	25
IV Sample Normalized Power, Node 3	25
V Sample Power Ratios, Node 3	27

List of Symbols

D_c = Diameter of Radio Frequency Induction Coil

D_p = Diameter of the Plasma

ϵ_c = Current Coupling Effectiveness

ϵ_{ce} = Current Coupling Effectiveness

ϵ_{rp} = Radiation Power Coupling Effectiveness

ϵ_{ew} = Wall Loss Power Coupling Effectiveness

ϵ_{et} = Total Current Coupling Effectiveness

ϵ_e = Plate Power-Usefulness

ϵ_{et} = Plate Power-Usefulness

ϵ_{et} = Plate Power-Usefulness

ϵ = Power Ratio

ϵ_{ce} = Current Coupling Ratio

ϵ_{rp} = Radiation Power Ratio

ϵ_{ew} = Wall Loss Power Ratio

Contents

	Page
Preface	ii
List of Figures	iii
List of Tables	iv
List of Symbols	v
Abstract	viii
I. Introduction	1
Origin of Study	1
Statement of Problem	2
Experimental Approach	2
Possible Uses	3
II. Experiment	4
Description of apparatus	4
Gas supply system	4
Plasma-Generator	4
Colorimeter	4
Vacuum system	7
Coolant system	8
Temperature recording system	9
Support stand and scaffold	10
RF Power supply	10
Experimental Procedure	11
Pre-starting Checks	11
Starting procedures	13
Data Run	14
Physical appearance of plasma	15
Temperature profile	17
Operating Modes	20
Mode 2	21
Mode 3	21
Mode 4	21

Contents

	Page
III. Discussion of Data	23
Data Reduction	23
Data Representation	27
Data Accuracies	29
IV. Results and Conclusions	32
Plasma Operation	32
Temperature Profile	34
Power Measurements	35
Combining Parameters	36
Gas Flow	37
Gas Composition	38
Plate Voltage	38
Interjacket	39
V. Recommendations	41
General	41
Plasma-Generator	41
Gas Injection Rate	41
Tube Diameters	42
Starting Conditions	43
Cells	43
Interjacket	43
Coolant Temperature Measurements	44
Plasma Temperature Measurements	44
Radiation Power Measurements	45
Energy Balance	47
Supersonic Heating	48
Duty Cycle as a Parameter	49
Summary	51
Bibliography	52
Appendix A	53
Figures	54
Vita	71

Abstract

A rf, electrodeless plasma-generator was developed which operated at peak plasma powers of 50 kw. The plasma was vortex stabilized, and was contained within a water-cooled Vycor tube. Power was measured calorimetrically. Radiation power was measured by alternately using clear water and water made opaque with India ink to cool the Vycor tube. A model temperature profile was deduced from spectrographic measurements transverse to the plasma axis. Maximum plasma temperatures were shown to exist in a thin cylindrical sheath near the plasma surface, with relatively cooler temperatures existing at the center-line gas back-flow. Effects of changing gas flowrate, gas composition, rf power, and Vycor tube diameter on the effectiveness of the energy coupling mechanism are shown.

A STUDY OF THE
INDUCTIVE-COUPLED PLASMA
ERIK L. PFENDER

1. Introduction

In inductively-coupled plasma, the plasma is heated by a vertically ionized gas by electrical currents. The gas is inductively coupled to a radio frequency (rf) current source. This method of plasma production is capable of generating plasma-free, β (the ionization fraction) is characterized by direct-current and alternating-current arcs. These arcs are initiated by electrode erosion caused by the direct contact between the electrodes and the arc.

Inductively-coupled plasmas are "electroless arcs" and there is no direct contact between the plasma and the rf power supply.

origin of the study

E. Pfender of the Institut für Plasmaphysik, Stuttgart-Degerloch, western Germany, initiated this study while he was engaged in research work at the Boehringer Ingelheim Research Laboratories (AHL), Wright-Patterson AFB, OH, at the suggestion of H. Boehnken, Chief of the thermodynamics laboratory, AHL. E. Pfender is interested in this plasma because it provides a possible source of electrons, ions, and neutral atoms which are in local thermal equilibrium (Ref. 2: 824), while H. Boehnken was primarily interested in the energy transfer characteristics exhibited by this plasma coupling mechanism.

Statement of Problem

The objectives of this study were (1) to operate a stable plasma at atmospheric pressure at 400 kilocycles (kc) with a sustained, high-power operation capability, (2) to determine the temperature profile of the plasma as a function of the plasma radius, $T(r)$, (3) to measure the power transferred to the plasma, and (4) to determine parameters important to the energy coupling mechanism.

Experimental Approach

The plasma was contained in a water-cooled Vycor tube (Fig. 1), and was stabilized in the vortex flow resulting from tangential gas injection in the manner prescribed by J. B. Reed (Ref. 2: 822).

The temperature profile, $T(r)$, was deduced from intensity profiles, $I(x)$, of the lambda 7635A I and lambda 4865A II spectral lines obtained by spectrographic scans transverse to the plasma axis.

The total power transferred to the plasma was determined by measuring the power the plasma transferred to cooling water. Radiation power was measured by circulating an opaque coolant instead of clear water about the Vycor tube which contained the plasma (Fig. 2).

The parameters varied in this study were rf power delivered by the power supply, gas flow, the diameter of the Vycor tube containing the plasma, and the gas composition. The rf power was varied by changing the plate voltage of the power supply, and the gas composition was changed by mixing helium and argon.

Possible Uses

As stated by Reed, (Ref. 2: p24),

"It is still too early to say what the capabilities and limitations of inductive plasma generation are. We have used the plasma torch to grow single crystals of refractory oxides, and oxygen-containing plasmas will melt aluminum oxide ($mp = 2700^{\circ}K$). The temperatures achieved in the plasma will depend ultimately on the power available and the nondestructive confinement of the plasma. Presumably, the induction plasma will find use wherever the dc plasmas are used, from measurement of spectral transmission probabilities to preheating gases for use in hypersonic wind tunnels."

In addition to preheating the gases for use in hypersonic wind tunnels, start-up temperatures attainable in hypersonic wind tunnels can be increased by heat addition in the supersonic flow section using an induction-coupled plasma.

II. Experiment

Description of Apparatus

Part of the experimental apparatus is shown in Figure 3. In the background is the rf power supply. Starting at the extreme left, the apparatus seen is a portion of the gas supply bottle, the vacuum pump and vent, the vacuum pump shut-off valve, the exhaust valve, and the vacuum system pressure gages. The pressure gages are mounted on the support stand. Above the support stand the calorimeter jacket, plasma-generator, and the support stand scaffold are seen. Behind the calorimeter jacket two meters are seen, which were not pertinent to this study. The drapé covers other equipment which was not pertinent.

Gas Supply System. The argon and helium used in this study were supplied by the Burdett Oxygen Company, and contained no more than one percent impurities by volume. Gas flows were measured by Airco Dual Range Flowmeters for argon, style number 805-1601. These meters were calibrated from 1 to 126 standard cubic feet per hour (scfh). Gas flows in excess of 126 scfh were measured by using the meters in parallel. Helium flowrates were obtained from the argon flowmeter readings by use of conversion graphs furnished by Airco.

Plasma-Generator. The water-cooled plasma-generator was made in four pieces, the top and bottom end-pieces, and the inner and outer tubes (Fig. 4). The end-pieces were made of brass, the outer tube was Pyrex, and the inner tube was Vycor. Standard rubber O-rings coated with high vacuum silicone grease provided the seals between the end-pieces

and tubes.

The top end-piece contains the gas inlet, the gas injection plate, and the coolant outlet. In the gas injection plate are eight 0.075-mm-diameter holes equally spaced on a two-inch-diameter circle. The holes are 0.075 in. off-center to the edge of the injection plate. As the gas enters the lower tube through these holes, the laminar-stabilizing vortex is formed. The coolant outlet is a tube of 3/8-in. copper tubing.

The bottom end-piece contains the bottom exhaust port, the coolant inlet, and the coolant manifold. The hot gas exhaust axially through a 7.0-mm-diameter port, and a piece of 3/8-in. cop or tubing provides the coolant inlet. The coolant enters and leaves the coolant manifold tangentially to prevent laminar flow from forming in the coolant as it circulates between the inner and outer tubes. The coolant manifold is formed by two tubes in grooves in the bottom end-piece. The coolant leaves the coolant manifold through the annulus formed by the inner tube and the 7.0-mm-diameter tube that forms the top of the manifold. This narrow exit annulus (1.7-mm wide) holds the coolant between the tubes from the no-skip effect at the coolant inlet. This permits an upward axially flow pattern, free of stagnation areas, to exist between the tubes.

The tubes are mounted co-axially between the end-pieces. The inner tube is a Vycor tube 18-in. long with a nominal 75-mm outside diameter. Vycor was required because the inner tube must be capable of supporting a severe temperature gradient. On many occasions it was

observed that while the outer surface of the Tycon tube remained at water temperatures, the inner surface was flowing red hot. The outside diameter is listed as a nominal 75-mm because variations in this diameter of plus or minus one or two millimeters are common, and the tubes are often cut-off-round. Because of these imperfections, the ends of the Tycon tubes must generally had to be sized before they were used.

The outer tube was a Tycon tube 1/2-in. long with a nominal outside diameter of 75-mm. The outer tube carries the axial compressive loads which are applied to hold the launch-tee together. The end-tees are constructed in such a way that no axial or reactive loads can be applied to the inner tube. This was done to prevent possible breakage of the inner tube by the combined effects of axial compression, thermal stresses, and hoop stresses caused by the reaction of the coolants.

Standard rubber washers were used to provide a seal between the end-tees and the inner and outer tubes. Two -pnts were used at each seal to improve the reliability of the seal. Rubber washers were used to prevent "direct" contact between the ends of the tubes and the end-tees to prevent chafing. The bottom end-tee is supported by the calorimeter and in turn provides the seal between these two parts.

Calorimeter. The calorimeter consists of a water-cooled jacket and two interior coils of copper tubing (FIG. 7). The water enters the outer shell of the jacket, flows up the outer shell, down the inner shell and then leaves the jacket. The cooling water next flows through the ascending coil of copper tubing, which is wrapped around the descending coil of copper tubing, and then through the descending coil and

out of the calorimeter. The coils of copper tubing were modifications made to extract the equivalent, and represent the simplest change that could be made. An exhaust joint in the exhaust pipe was separated and the cooling coils were inserted into the exhaust pipe. The cooling arrangement that resulted was not ideal, but it was adequate. The exit orifice of the exhaust pipe was located after the gas left the calorimeter, and the heat loss was probably due to the exhaust gases at this point (approximately 2.3 K/min at 1 ps). After the gas leaves the calorimeter, it can be directed to the atmosphere or to a vacuum pump.

The vacuum system. The vacuum system used to maintain an evacuated tube assembly was built, patent number 26,3315. This is a single-stage, rotary-vane, oil-sealed pump. The 200 cu in oil bath is able to maintain the pressure in the plasma generator to 1.00 x 10⁻³ torr (0.001 absolute) (20 torr), after no-flow conditions.

Pressure readings were read on a vacuum pressure tube calibrated from 2-mm to 10-mm Hg. The range of interest was below 1.00 mm Hg. If pressure readings below 1.00 mm Hg were attained, it failed to get satisfactory seals in the plasma-generator, and a start could be made. The plasma was not operated in a vacuum other than during starting. A second pressure tube in the system, which read pressures above and below atmospheric, in inches of mercury, was used to determine the appropriate time for opening the exhaust valve. The exhaust valve was opened when the pressure was sufficiently below atmospheric pressure.

Coolant system. The coolant system consisted of a coolant supply, the plasma-generator, the calorimeter, flowmeters, and connecting lines.

The primary coolant was tap water, but an alternate coolant supply was available for use in the plasma-generator. The alternate coolant was "black water" and was used to measure radiation power. The black water was a mixture of Carter's India Ink, tap water, and aqueous ammonia. The approximate proportions used were 30 gallons of water, three pints of India Ink, and one pint of ammonia. The Ink was added to the water until the plasma was no longer visible through the plasma-generator, and the ammonia was added to prevent the Ink from separating out of the water.

During operation, the black water was recirculated through a galvanized drum. The water which flowed through submerged cooling coils in the drum received heat from the black water as it recirculated. The recirculating pump will deliver 1100 pounds of water per hour at 24.5 rpm, fifteen min. 400 pounds per hour less water and six psi less pressure than the tap water supply provided. The higher flowrate for tap water was used to inhibit nucleate boiling in the plasma-generator, because nucleate boiling leaves mineral deposits on the inner tube which interfere with radiation measurements.

Selector valves in the plasma-generator coolant lines permitted a shift to black water without the necessity of stopping the plasma. A bypass line was put in the black water system to permit operation of the recirculating pump at any time.

Coolant inlet pressure was monitored during the runs. In general, the black water pressure remained constant, but occasional 5 Hz frequency fluctuations were noted. The top water pressure was often varying up and down as much as two psi several times a minute.

Coolant flow to the plasma-generator was measured by four Fisher and Porter strobilite rotameters in parallel, and water flow to the exhaust water was measured by a Fisher and Porter flowmeter. The rotameters and flowmeter were accurate to the nearest five pounds per hour. The rotameters could not be read when operating with black water, however, so it was necessary to turn off the black water and select the clear water to read the rotameters to allow the new flow to settle and stabilize (10 sec). Thereafter, the black water flow was assumed constant, which appears to be a good assumption based upon the constant black water outlet pressure.

Temperature Recording System. The temperature recording system consisted of a J-type thermocouple, a cold junction, and a continuous recording galvanometer. The recording galvanometer used was a Honeywell Visicorder, Model 966-1590III. The system was calibrated at ice bath temperature, bottom water temperature, and at 90°F and 150°F. The system was linear over this temperature range, with an average response of 0.5°F per inch. The Visicorder traced a ten-line-per-inch scale on the tape, and the temperature traces were about 1/20-in. wide. The deflection of the center of the temperature trace was read to the nearest 1/40-in. Recordings were simultaneously made of the coolant inlet and outlet temperatures, and of the exhaust

and temperature after the gas left the calorimeter.

Support stand and scaffold. The calorimeter was mounted in the support stand (Fig. 3). The calorimeter supported the bottom of the plasma-generator, and the support stand scaffold restrained the top of the plasma-generator. The restraining force applied to the top of the plasma-generator was necessary to hold the plasma-generator together because of the pressure of the coolant in the plasma-generator. The force on the top end-plate caused by this pressure was strong enough to cause the optional wooden cross-bar of the scaffold to bend and thus allow the top end-plate to move. For this reason, an aluminum channel was used to reinforce the cross-bar, and then the restraining force was adjusted so that the top end-plate did not visibly move when the coolant was turned on. The outer tube of the plasma-generator is required to carry this load, and also the load resulting from the vacuum in the inner tube, before the coolant is turned on.

RF power supply. The rf power supply was a Westinghouse power oscillator rated at 200 kw at 4.0 Mc. The power output of this oscillator could be controlled by selecting one of the nine discrete plate voltages available, and then selecting a duty cycle. The plate voltage could not be changed until the power supply was operating, however, the duty cycle could be varied at any time from 0-100%. At duty cycles less than 100%, the rf power was delivered in pulses of varying lengths depending upon the duty cycle selected. The pulse rate was 360 per second. A duty cycle of 50%, then, resulted in pulse lengths of 1/720 second. A 100% duty cycle was used for this study, except during starting.

Experiments in Socialism

The experimental conditions had to be repeated for the three tanks tested. From these trials plus the (1) starting line, (2) starting lines, and (3) line of no tolerance, the tanks covered under one of the following conditions: (a) start of race at the starting line, (b) start of race at the starting line, (c) starting line, and (d) start of race at the only tolerance line, unless specified otherwise. The results of the starting line experiments are given in Table I.

the *Journal of the Royal Society of Medicine* will be received.

If the vacuum pump is not functioning, the coolant system is turned on, and a check is made for leaks. Eventually, water will seep into the inner tube even though the vacuum checked below 1 centimeter.

When this occurs, it is an indication that a leak has occurred and the well form where the water enters the filter system. Small leaks of this nature can often be stopped by tightening the well screen and thereby reducing the headloss. If this effort fails, it is necessary to disassemble the back-filtering well and to inspect the screen for different sizes.

If no leaks are apparent, the sand filter inlet pressure is raised to 20 psi, and the filter system is operated for a period of time. The flow to the filter system should be approximately 1000 gallons per hour, and the flow to the sand filter should be about 300 gallons per hour. The sand filter inlet pressure is then reduced to obtain the filter required to produce the required flow.

No pressure is applied to the sand filter in the filter system, but a portion of the water will be forced by osmosis through the sand of the sand filter system, thereby the amount of water that can be removed by the filter will be dependent on the head loss. This, after the filter system exhibits proper operation, is to be gradually released until the filter inlet pressure is no longer apparent.

Any amount of the filter inlet pressure is determined by the amount of pressure drop.

With the completion of the sand filter, the sand filter and filter system operation are assured. However, the filter system will be checked for head loss daily or according to a schedule. The filter will be checked for a steady, reduced flow, and then the head loss will be measured and the filter system for a data run.

Starting Procedure. The starting procedure is not included in the data run section because special attention should be given to this critical portion of the plasma operation. The plasma is started in an argon atmosphere at an absolute pressure less than 10⁻⁴ mm. The required electron current for a sustainable plasma starts may be obtained at lower rf power settings, but requires the availability of lower tube fluorine. The initial acceleration of the plasma is then to proceed the same, as it does after operation at the resonance, but the rf power is too high.

When the starting procedure has been reached, the rf power supply is turned on, and the rf supply is gradually increased until a hole is taken through the tube fluorine. At this time, the valve to the vacuum tank is turned off, because the argon is no longer needed and because this method leads to a more rapid pressure build up in the plasma. The rf supply valve is now turned on, and the valve of the flow meter left, a brilliant blue glow will be observed. The next step is ten seconds to the most critical period of plasma operation. The flow is gradually increased to about 75 cc/s, while the power is gradually increased to that of the pressure rise associated with the gas flow. Should the power be increased too slowly, the plasma will extinguish; if the power is increased too rapidly, the plasma will contact the tube with sufficient energy to effeclor it. This acceleration is permanent and precludes the use of the tube in radiation measurements.

The danger of discoloration rapidly decreases (due to plasma contraction) as the pressure and gas flow increase. As soon as the plasma contraction is noticed, the rf power may be increased fairly rapidly to a duty cycle setting of approximately 50%. Meanwhile, a close check on the plasma pressure is maintained, and as the pressure rises towards zero volts, the exhaust valve is opened. When this task has been accomplished, the start-up procedure is complete.

Data Run. The data run begins when the gas flow is increased to the maximum value of 25 scfm attainable, and the duty cycle is adjusted to 100%. The duty cycle remains on 100% for the remainder of the data run, while the gas flow is reduced in 25 scfm increments, until a flow of 10 scfm is reached. As soon as temperature equilibrium for each flow rate is indicated by the traces on the Waterorder tape, the tape is stopped with the no-state gas flow, and all meters are read. The meters read are the rf power supply plate voltmeter and plate ammeters, and all the water flowmeters.

A lower limit of 10 scfm on the gas flow was established because at flows less than 10 scfm, coolant bubbles become substantial enough to cause mineral deposits to form on the laser tube, which interfere with radiation measurements.

After readings for a gas flow of 100 scfm are taken, the gas flow is increased to its maximum value as before, and the plasma-generator coolant supply is switched to black water. The coolant flowmeters must be read as soon as the coolant flow indications stabilize. There is

sufficient clear water in the coolant system ahead of the black water to allow the stabilized flow-indicators to be read, before the flow indicators are obscured by the black water. The black water flowrate is assumed constant for the regulator of the data (a). This assumption is reasonable since the black water and its pressure remains constant except for occasional fluctuations of very frequency. Fluctuations of plus and minus 1/2 psig. The origin of these fluctuations is unknown, however, the fluctuations did not appear to effect coolant flowrate.

With the exception of the assumed constant values of black water flow, meter readings are obtained at 25 sec flow increments as before. After the final set of readings are taken, the rms flow is increased to maximum value, and the duty cycle percentage is decreased, prior to turning off the rf power supply. This was done to cool the inner surface of the inner tube gradually enough to prevent post-operating tube cracks, which result from residual stresses caused by rapid cooling.

After the rf power supply was turned off, the clear water coolant supply was again selected, thereby flushing the black water from the coolant lines.

Physical Appearance of Plasma

The plasma first appears as a brilliant blue white discharge, in the vicinity of the rf induction coil, the instant the argon gas flow commences during the starting procedure. The plasma appears to extend out to the Vycor tube when operating at this low pressure. As the pressure and gas flow increase, the plasma contracts so that the

luminous gases no longer appear to contact the tube wall. The plasma is now shaped as a cylinder five to six inches in length and roughly centered in the rf coil area. This general shape is maintained until the gas flow approaches 60 secfh. At this gas flow, the top edge of the plasma intermittently extends up to the injection plate in the top end-plate. As the gas flow is increased to 70 secfh, the back-flow of gases up the center of the tube becomes strong enough to cause the top edge of the plasma to become permanently extended. The diameter of the extended portion of the plasma is largest level with the top of the rf coil, and is smallest at a point about two inches below the injection plate (Fig. 4). At this point the plasma begins to diverge toward the inlet holes in the injection plate. Further the increase in gas flow, the bottom edge of the plasma extends downward slightly. Below the bottom coil, the brilliance of the plasma fades very sharply into a ragged-edged tail-flame approximately one inch long.

This description is representative of typical plasma operation. The dimensions of the plasma were not measured, and all stated values are approximations. Further, the dimensions of the plasma, and the gas flows at which plasma extension occurs are strongly dependent upon the rf power level. More important than the exact dimensions of the plasma are the changes in appearance of the plasma which result from changes in rf power and gas flow. Within the range of rf power and gas flow used in this study, increasing the rf power increases the diameter of the plasma and increases the length of the tail-flame, while increasing the gas flow decreases the diameter of the plasma, and increases

the length of the tall-flame. The changes due to changing rf power were observed by stopping the rf by cycle. After the rf power and gas flow were set for a data run any changes in the brilliancy of the plasma were too subtle to be detected by eye. Due to the intense brilliancy of the plasma, it was normally observed to be a dark green color.

Current profile

A method for finding the temperature profile of an ionized plasma is exhibited by C. C. Mack, *Appl. Phys. 11: 719*. In brief, it is based upon the temperature dependence of the normalized relative intensities of the interelectrode current (at 1000 K) and the total electron current (at 1000 K) $I_e(x)$. The observed intensities of these three along a line, $I(x)$, are converted to the interelectrode current fractions of the radius, $J(r)$, by the following equation (Appendix A). The first differential coefficient is to be removed to x .

$$J(r) = -\frac{1}{\pi} \int_r^R \frac{N'(x) dx}{\sqrt{x^2 - r^2}} \quad (1)$$

Figure 6 shows the results obtained by inverting observed $I(x)$'s to radial distributions, $J(r)$'s using this formula, and then normalizing each curve with respect to its maximum intensity. This figure clearly shows that $J(r)$ has a more pronounced dip at r equal zero, than does $I(x)$ at x equal zero. The temperature profile, $T(r)$, may now be plotted by taking the normalized relative intensity of one of the

spectral lines from Figure 6 for a particular radius, and obtaining the corresponding temperature from Figure 5. At this point, it is well to note that an ambiguity exists when using a single spectral line to determine temperature. With a normalized relative intensity of 0.85, it is possible to obtain values for temperature of either 14,000°K or 16,500°K. This ambiguity is solved by the presence of a measurable intensity of Lyman 4P0/4L1, which indicates temperatures above 15,000°K; or by the absence of this line, which indicates temperatures less than 14,000°K.

The investigation of the temperature profile of the plasma center study were not complete. However, sufficient preliminary investigations were made to justify certain conclusions concerning the temperature distribution.

The Intensity of Lyman 4P0/4L1, $I(x)$, was recorded with a monochromator at the center-line. The recorded $I(x)$ showed maximum values off the center-line (Fig. 7). The recorded maximum intensity and the center-line intensities increased as a result of the first power increases. The lower level was raised with a relative increase in power producing no increase in the recorded maximum intensity. At this point the spread between the off-center intensities tends to increase, and the center-line intensity begins to stabilize. These off-center peak intensities were now inter related to the location of the 15,000°K isotherm. Since the center-line intensities as $I(x)$, were always less than the off-center maximums, even when these off-center

maxima could not be identified with the 15,000 ft. soother, it was concluded that the center temperature was less than 15,000°K. If, however, these low center-line intensities were indicative of temperatures above 15,000°K, the temperature would have to be 10 excess of 15,000°K. At this temperature, the 1660 Å (D2) line should show a very little, if any, center-line reversal. The temperature of the plasma at the center-line reported the temperature did not exceed 15,000°K. The presence of the 1660 Å (D2) line was detected in the plasma, but only very faintly, and its constant intensity normal to the plasma, also strongly indicated no reversal of the existence of a temperature above 15,000°K. It is very likely, although near the edge of the plasma, that the center-line temperature is less than 15,000°K.

These optical observations, in addition to the other proposed physical characteristics of the plasma, indicate the first proposed characteristic is that with effect of the current, and to be transferred to the plasma, is a modification in the form of varying electrical conductivity, and change in the form of varying temperature. The second proposed characteristic is that the current reversed its flow in the center of the plasma, toward the left, effecting the conductivity, and the velocity, is modified only slightly by the presence of the plasma. The existence of straight boundaries in the plasma center, and the presence of the high viscosity exhibited in plasma whose temperature are above 15,000°K.

The plasma is returned then to having its maximum temperature existing in a thin cylindrical shell near the outer limit of the plasma, with a strong reverse flow of relatively cool gases up through the

center of the plasma. These findings are contrary to the findings of T. B. Reed who concluded that the highest temperatures exist at the plasma center (Ref. 1: 223). The plasma investigated by Reed, was operated at a frequency of 4 megacycles at atmospheric pressure, using low ion fluencies, the anode tube had an outside diameter of 26 mm.

Operating Modes

Four modes were operated in the tubes, as shown in Table I. As the voltage and polarity concerned, Mode 1 was to be the standard mode for use in ion sources, and the other modes were to be different from Mode 1 in only one parameter. However, the plasma would not start in Mode 1, probably due to anode. However, the plasma would not start in the 3rd mode, due to the negative of the anode voltage (- V); and plasma operation was only possible at a plate voltage of 7.6 kv, so the 3rd mode was not used. Mode 1 was chosen as the standard mode because operation is reliable and the simplest. Laboratory techniques used in this study resulted from the experience gained while operating in Mode 1.

Table I
Operating Modes

Mode	Plate Voltage (kv)	Gas (%, by Volume)	Inner, i.e. cathode diameter
1	7.6	1.0, n	75-mm
2	8.2	1.0, n	75-mm
3	10.1	1.0, n	75-mm
4	8.2	53, n 47, %	75-mm

Note 2. Operation in Note 1 was to show the effect of increasing the rf power available in a duty cycle of 100%. In particular difficulties were encountered in the operation in note 1; however, power control, light & startline, was more critical since the rf power was increased more rapidly with increasing duty cycle. Corrected to note 2 this is due to note 1.

Note 3. Operation in note 3 was to show the effect of operating the magnetron with a smaller tube, with the result that with the same rf, current & voltage, the magnetron, became difficult to extremely difficult to start. This was attributed to the smaller tube, which resulted in a more intense magnetic field. The magnetron was then modified to a larger tube, and the magnetron was then found to be more easily started. The smaller tube, as modified, was called a "short tube" and the larger tube, a "long tube".

On the basis of experience of note 3, the magnetron, modified from notes 1 and 2, was then again extended in the magnetron. Late in 1959, the magnetron was modified, and the tube, following the same also extended well down the tube, became rf matched, and a suitable extension tube, the magnetron tube, was made. The modification was verified.

Note 4. Operation in note 4 was to show the effect of fitting the magnetron with helium. Operation at low frequency volumes was desired, and operation with helium required a plate voltage of 6.2 kv to insure reliable operation. The fixture that was used in

this indicates approximately 40% change in volume. The change was started to increase and the change was arrested after the duty cycle had been subjected to 100%. The increase of the plateau which was 47% higher was not very different from the increase of a more normal change. However, the increase was still significantly larger, the plateau of the 100% increased plateau (47%) being 1.5 times the 100% initial plateau.

III. Discussion of Data

The discussion of the data is presented here under three headings; data reduction, data presentation, and data accuracies. In this manner, it is hoped that the reader will gain a feel for the problems involved using the experimental techniques outlined in this study.

Data Reduction

The recorded data were in the form of volts, amperes, and flow rates. These data were first converted into over units, kilowatts, and then tabulated as shown in Table II.

Table II
Sample Power Measurements, 'Mode 3'

Row	Gas Flow (scfh)	Q_w (kw)	Q_b (kw)	Q_c (kw)	P_t (kw)	P_f (kw)	P_e (kw)
1	175	9.14		3.93	147.0	120.0	27.0
2	175		12.98	4.02	152.8	120.0	32.8

The symbols used in the table are defined as follows:

Q_w - The power measured from the clear water used to cool the plasma-generator.

Q_b - The power measured from the black water used to cool the plasma-generator.

Q_c - The power measured from the cooling water in the calorimeter.

P_t - The plate power measured in the rf power supply when the plasma is operating.

P_f - The plate power measured in the rf power supply when the plasma is not operating, or idling plate power.

P_e - The excess plate power, which is the difference between P_t and P_f .

The first row of data was recorded during the clear water run and the second row recorded during the black water run. The difference in plate power between these two runs of 5.8 kw is larger than most differences recorded, but it serves to show the necessity of normalizing the data before any computation of the radial radiation power, Q_r , can be made.

The quantity Q_w is a measure of the power transferred to the walls by convection and that portion of the radiation absorbed by the clear water and the glass tubes. This portion of the radiation power was assumed negligible in comparison with either total radial radiation power, or convective power to the walls. The quantity Q_b is a measure of the sum of the power transferred to the walls by convection, Q_w , and the radial radiation power, Q_r . Q_r is radial radiation power that exists in the range of wavelengths for which Vycor, water, and Pyrex are transparent.

Note: The quantity Q_r will hereafter be referred to simply as radiation power. It is in fact a measure of radial radiation only, as the axial radiation power is absorbed by the top end-piece of the plasma-generator and the calorimeter. No attempt was made to measure the axial radiation power, but it is included in the measurement of Q_w and Q_b .

If we therefore subtract Q_w from Q_b , the difference should be Q_r . From Table II, the value for Q_r thus computed would be 3.84 kw. Implied in this computation is the assumption that all the additional power measured with the black water was radiation power, and no consideration was given to fact that the rf plate power was 5.8 kw higher during the black water run. This increase in plate power reflects an increase in rf power output of something less than 5.8 kw due to normal losses in

the rf power supply. In turn, there would be an increase in power transferred to the gas current. Note that the increased rf power output due to normal coupling is reflected between the rf coil and the plasma.

The problem, therefore, is to determine how much of the 3.14 kw is due to coupling, and how much due to the increase in rf power output. It is not necessary to know the power input to obtain the normalized coupling coefficient by subtraction.

The data were normalized and presented in Table III. Note the values for the four different plate voltage settings. Note also, E_b , and E_c are divided by the total power to a quasi-stationary value which will be called E_{b0} , E_{c0} , and E_{t0} , respectively. Values for E_{b0} are plotted in Figure 17. Table IV is the result of normalizing the data in Table III.

Table III
Normalized Power

Mode	Plate Voltage (kv)	P_t (kw)
1	7.6	72.0
2	8.0	77.0
3	10.1	120.0
4	8.2	77.0

Table IV
Sample Normalized Power, Mode 3

Gas Flow (scfh)	E_w (.)	E_b (.)	E_c (.)	E_t (.)	η_t (kw)
175	33.8		14.55	5.8	1.57
175		39.6	12.25	5.9	1.90

Σ_p is taken as the difference between Σ_0 and Σ_N , and is assumed to be unaffected by the different values of I_0 . The validity of this assumption is open to doubt, but it appears to be a better first approximation than assuming that ϵ_p remains constant during the increase in I_0 . The values for ϵ_p listed in Table III are found by multiplying ϵ_p by the appropriate I_0 . This was done for the sake of comparison with the non-normalized value for ϵ_p of 3.2% Σ_0 . It is also apparent from Table IV that two values for Σ_0 can be obtained at each gas flow. Hereafter when a value is given for Σ_0 , whether it be in text, table, or graph, the value given will be the average of the two values of Σ_0 for that gas flow. From Table IV, the value of Σ_0 is 13.6% for a gas flow of 175 scfm.

The quasi-efficiency nature of the quantity Σ was mentioned, without discussion, before. Σ , as defined, is the percentage of excess rf power which goes to the plasma. The percentage of additional rf power which goes to the plasma would be of more interest to this study, but no means of measuring rf power was not found. It is possible to say, however, that the amount of rf power available from this power source to operate the plasma is less than ϵ_0 , and it is not likely that all of this excess plate power is converted to rf power. Therefore, the values found for Σ will be conservative estimates of the coupling efficiency between the rf coil and the plasma. An item of interest, in addition to power conversion efficiencies, is the manner in which the power that goes to the plasma is distributed between the wall, radiation,

and the calorimeter. After ϵ_w , ϵ_p , and ϵ_c are found, they can be summed to form a total effectiveness, ϵ_t . Let the ratio of ϵ_w , divided by ϵ_t , be defined as R_w . Similarly, define R_p and R_c . These ratios show the distribution of power within the gas, as illustrated in Table V.

Table V
Sample Power Ratios, Mole 3

Gas Flow (scfm)	R_w (%)	R_p (%)	R_c (%)
175	63.8	10.9	25.3

Data Presentation

The data are presented in terms of the power coupling effectiveness, ϵ , and the power distribution ratio, R , vs. gas flow in Figures 10 through 16. The results on the ϵ_w , ϵ_b , and ϵ_c vs. gas flow graphs (Fig. 10 and 12) were obtained by normalizing ϵ_w , ϵ_b , and ϵ_c with respect to ϵ_t . The curves on these graphs represent the best fit to the data points by a second order (parabolic) curve. However, there is good argument for use of a third order (S-shaped) curves for ϵ_b , Node 2, and for ϵ_w , Nodes 2 and 3, based on the number of data points and their distribution. The type curve chosen to represent a series of data points should be based upon the exactness to which each data point can be located, as well as to the number and distribution of the points. If high confidence in the location of each data point is justified, a curve which closely fits all the data points can be drawn. If, however,

the possible variation in the exact location of a data point is large, then a lower order curve which tends to average out the point location uncertainties is more reasonable. The exact locations of the data points for E_b and E_w are not known with sufficient accuracy to justify more than a second order curve.

The feet attached to each end of these curves show the possible vertical displacements of the data points based upon the probable error in reading the coolant temperatures of plus or minus one degree Fahrenheit. These vertical displacements are essentially constant for all data points along that curve, and this display method was chosen over attaching the feet to each data point to prevent excessive cluttering of the graphs.

After the curves for E_b , E_w , and E_c were plotted, the difference between the E_b and E_w curves was drawn as the E_r curve (Fig. 11), and the sum of the E_b and E_c curves was drawn as the E_t curve (Fig. 13). The data dispersion which is inherent in the process of subtracting at each data point, and then plotting, is shown quite well in the plots of the data for E_r . The data points shown result from the subtraction of E_w data points from E_b data points. The subtraction technique will always produce this type of dispersion whenever the data are not perfectly smooth. The probable vertical displacement of points on the E_r curves was taken as $(2)^{1/2}$ times the average displacements for the E_b and E_w curves since these displacements are close to being equal.

The curves for R_w , R_r , and R_c result from dividing the E_w , E_r , and E_c curves by the E_t curve. In this manner, the normalizing quantity

P_e is eliminated, and the resulting quotients, Q_w/Q_t , Q_r/Q_t , and Q_c/Q_t , are the power distribution ratios, E_w , E_r , and E_c (Fig. 14, 15, and 16).

Data accuracies

The only significant source of error in the data results from the low accuracy to which the coolant temperature rises can be determined. By reading the deflection of the center of the temperature trace to the nearest $1/40$ -in., the probable error in temperature measurement is approximately plus or minus one degree Fahrenheit. The following example illustrates the consequence of such an error.

For a typical coolant flow of 2500 pounds per hour, an error of plus or minus 0.732 hr may be expected in the value for Q_w . The resultant errors in E_w , from errors in power of this size, range from plus or minus 2.5% to plus or minus 0.9%. That is to say E_w equals 40% plus or minus 2.5%. For E_b , the errors due to inaccurate temperature measurement, range from plus or minus 2.2% to plus or minus 0.8%, which are slightly less than errors for E_w due to the lower black-water flowrate. The errors in E_r will contain the errors in E_w and E_b . Since the errors in E_w and E_b for a particular operating mode and gas flow are approximately equal, the error in E_r was taken as the $(2)^{1/2}$ times the numerical average of the errors for E_w and E_b . The range of errors thus computed for E_r are from plus or minus 3.3% to plus or minus 1.2%. Except for some variations in coolant flowrates, the errors in E_w , E_b , and E_r due to an error of plus or minus one degree Fahrenheit, are inversely proportional to the normalizing quantity, P_e . Other errors

result from the accuracy to which the coolant flowmeters, plate voltmeter, plate ammeters, and gas flowmeters can read, and from the failure to remove all of the cover from the gas in the calorimeter.

The two plate ammeters can be read to the nearest 0.1 ampere, and the plate voltmeter can be read to the nearest 0.1 kw. The inherent error here is plus or minus 0.035 kw which is insignificant when compared with the lowest value of P_e , which is 27 kw.

The Airco flowmeters are stated to be accurate within five percent, and they can be read to the nearest one scfh. It is assumed that any inaccuracies in the flowmeter are distributed over the whole range of the flowmeter. This type error will be shown as a scale error on the graphs, without appreciably changing the general appearance of the curves. The inaccuracy in reading the flowmeter would show as a horizontal displacement of a data point on the graph, however, a horizontal shift of one scfh would be hard to detect on the scale of 50 scfh per inch.

The largest amount of power remaining in the gas as it left the calorimeter was on the order of 0.03 kw. Had the calorimeter been totally effective, this power would add to Q_c . Since the smallest value for Q_c was 2.42 kw, the error in neglecting the power remaining in the gas is acceptable.

The water flowmeters could be read to the nearest five pounds per hour, or to within two and one-half pounds per hour. This error in coolant flow can lead to an error in power measurement up to 0.06 kw

depending upon the coolant temperature rise. The largest coolant temperature rises were in conjunction with power measurements on the order of 30 kw, so that this error is also acceptable.

IV. Results and Conclusions

Before presenting the results and conclusions, it is necessary to fix in the mind of the reader exactly what was measured during this study, and what the purposes of the study were.

The quantities \dot{Q}_w and \dot{Q}_b represent the power transferred to the coolant as it passes through the plasma-generator. The quantity \dot{Q}_c represents the power transferred to the coolant in the calorimeter.

\dot{Q}_w is composed of three terms; a wall loss term, a radiation term, and a first loss term. The wall loss is the power transferred by convection to the wall in the area of heat addition to the plasma. Since the plasma extends up to the injection plate, some wall loss is experienced there also. The radiation term is composed of the radiation absorbed by the coolant, the outer Lexan tube, the inner Tycon tube, and the top and bottom end-plates. The first loss term represents power transferred to the wall which was available in the gas flow as enthalpy after the gas left the area of heat addition.

\dot{Q}_b is composed of the same terms as \dot{Q}_w with an additional radiation term. This additional term represents the radial radiation power absorbed by the black water.

\dot{Q}_c is composed of two terms. The first term represents the power available in the gas flow as enthalpy after the gas leaves the plasma-generator. The second term represents the radiation from the plasma which is absorbed in the calorimeter. For the most part, this radiation

is axial radiation, but at high gas flow in small diameter tubes, the visible plasma could extend down into the calorimeter, in which case some radial radiation would also be measured.

The definitions for Q_r and Q_c need not be further expanded. Q_r remains the difference between Q_b and Q_w , and represents the difference between the total radial radiation and that portion of radial radiation which is absorbed by the plasma-generator, clear water, and the calorimeter should the plasma extend that far down. The total power transferred to the gas, Q_t , remains the sum of Q_b and Q_c .

The normalizing quantity, P_e , is the difference between a varying total rf power supply plate power, P_t , and the constant value of idling plate power, i.e. when a constant duty cycle is chosen, no control can be exerted on P_t , as the rf power supply automatically adjusts P_t in response to the load placed upon it. Since P_e differs from P_t by a constant, the variation of P_t with gas flowrate can be deduced from the plot of i_e vs. gas flow (Fig. 17). Refer to Table III for values of P_t .

The normalized quantities, E_w , E_r , and E_c represent a percentage of P_e , and therefore show how much of P_e was effectively transferred to the wall, to radiation, and to the calorimeter. When each of these characteristics is divided by their sum, E_t , the ratios R_w , R_r and R_c are obtained. These ratios show the percentage of the total power transferred to the plasma that goes to the wall, to radiation, and to the calorimeter.

In general, E_t did not vary greatly with gas flow (Fig. 13). Therefore, if either E_u , E_T , or E_c shows a strong variation, one or both of the other parameters must make compensating variations. Further, the relative constancy of E_t insures that increases or decreases in E_u , E_T , or E_c , are reflected by corresponding increases or decreases in R_u , R_T , or R_c . For this reason, the results and conclusions will be discussed in terms of E_u , E_T , E_c , and E_t only.

The objectives of this study were (1) to operate a stable plasma at atmospheric pressure at 400 kc with a sustained 5-kw-power operation capability, (2) to determine the temperature profile of the plasma as a function of the plasma radius, $T(r)$, (3) to measure the power transmitted to the plasma, and (4) to determine parameters important to the energy coupling mechanism.

Plasma Operation

Using the techniques described in this study, a stable plasma was operated at 400 kc at atmospheric pressure. No endurance runs were made, however, the plasma has been continuously operated for forty minutes during some data runs which included peak plasma powers up to 52 kw. With a modified injection plate to prevent injection plate damage, and heat resistant seals to prevent seal deterioration, the plasma is believed capable of continuous operation at the 50 kw power level at gas flows above 100 scfh, in a 75-mm Vycor tube. Stable operation of the plasma was concluded on the basis of apparent constant plasma geometry, and stationary values of coolant temperature indications during operation at constant gas flow.

Temperature Profile

Although temperature profile measurements were not complete, the existence of a temperature of 15,000K near the outer surface of the plasma was verified, and a model temperature profile was deduced. The deduced temperature profile shows the highest temperatures occurring in a thin cylindrical shell near the outer surface of the plasma, and relatively cooler center-line temperatures existing in a reverse gas flow.

Power Measurements

The techniques used to measure power were only partially successful. The margin for error in determining the coolant temperature rise was unacceptable for so critical a measurement. This fault coupled with the shift in P_e between the clear water and black water runs, led to excessive data dispersion which in turn prevented obtaining point-by-point radiation power values by subtraction of the point values for Q_w and Q_b . Q_w and Q_b were normalized with respect to P_e and the results plotted as E_w and E_b vs. rms flow in sefh. A smooth curve for E_w was then drawn and subtracted from the smooth curve drawn for E_b . This yielded smooth curves for normalized radial radiation power, E_r . The usefulness of radiation values obtained in this manner rests on the validity of the averaging processes inherent in normalizing data and plotting smooth curves. In consideration of the limitations imposed by possible data accuracies and experimental techniques used in this study, the information displayed on all graphs should be viewed as

first approximations of actual values and trends.

The black water technique as applied in this study is very useful as a means of determining total plasma power. Better measurements of radiation power would be possible with the use of an improved black water which did not leave deposits on the inner tube. This innovation is discussed under "Recommendations". With the use of an improved black water, this technique of measuring radiation power should yield useable radiation power data without the necessity of first normalizing the data.

Coupling Parameters

The controlled parameters were rf power supply plate voltage, inner Vycor tube diameter, gas composition, and gas flow, however, other implicit parameters were present. The implicit parameters appearing in this study are plasma pressure, vortex strength, rf power supply plate power, and plasma length and diameter. No control can be exerted over these parameters, as they are the natural consequences of varying the controlled parameters.

Conclusions concerning a coupling parameter must be supported by a reasonable quantity of data pertinent to the effects of that parameter. The preponderance of information gathered in this study directly concerned gas flow. For this reason, the effects of varying gas flow are well described. The effects of varying gas composition, inner tube diameter, and plate voltage cannot be described nearly as well due to the meager investigations made of each of these parameters.

Direct comparisons of the operating modes which contain these parameters as variables can establish a trend which would have some short range validity, but any long range projections made on the basis of these limited comparisons are of doubtful validity.

Gas Flow. The effect of increasing gas flow on all operating modes is similar, but somewhat varying in degree. For instance, a sharp decrease in E_y is noticed with an increase in gas flow for Modes 1, 2, and 3; but Mode 4 exhibits only a slight decrease in E_y . In general, the decrease in wall loss and radiation characteristics and the increase in the calorimeter characteristics with increasing gas flow can be attributed to the decrease in plasma diameter which occurs with increasing gas flow. Some lengthening of the plasma tail-flame is also noted with increased gas flow, but no significant increase in length of the highly luminous portion of the plasma was observed. As the plasma contracts, at high gas flows, wall losses are exhibited by the increased separation between the plasma and the walls, and the effective volume of radiating plasma is decreased, thereby reducing radiation losses. The reduction in radiating volume apparently offsets any tendency to increase radiation power through possible increased plasma temperatures. In the absence of temperature measurements to the contrary, it is believed that plasma temperature very likely decreases with the increasing gas flow due to the decrease in energy coupling to the restricted plasma volume.

The reduction of wall losses and radiation losses at higher gas

flows is reflected by an increase in power carried to the calorimeter by the flowing gases.

Gas Composition. The only gas used other than argon was a mixture of argon and helium. The mixture used was approximately 47% helium by volume, or about 8.9% helium by weight. This dilution of pure argon led to marked differences between the results of Mode 1 and Mode 2. The increase in wall loss characteristics and the decrease in radiation loss characteristics are respectively believed to be the result of the higher thermal conductivity and lower emissivity of helium. The calorimeter characteristics for these two modes are nearly equal, which suggests that the increased radiation losses were offset by equivalent increases in wall losses.

Plate Voltage. The effects of increasing plate voltage appear in the comparison of Modes 1 and 2. The changes experienced by raising the plate voltage were the least predictable of all changes resulting from varying the other parameters. It was earlier observed that an increase in rf power output increased the diameter of the plasma. During any data run it was also observed that as the diameter of the plasma increased E_t increased. These two bits of information seemed to point the way toward an increased coupling effectiveness at higher plate voltage settings. It was predicted that the higher rf power output, which would accompany the higher plate voltage setting, would increase the plasma diameter which would in turn increase E_t . The effect on E_t was just the opposite; E_t decreased. Q_w , Q_r , and Q_t , however, increased in Mode 2, but these increases were obtained at relatively higher increases

in ρ_e , so that δ_ρ , δ_T , and δ_ϵ decreased in Mode 2. The most unexpected result was that Q_c for Mode 2 was less than Q_c for Mode 1, for an increase in all power requirements was expected because of the increased rf power output.

No explanation of the decrease in δ_ϵ is offered. An examination of Figure 8 shows a decrease in electrical conductivity of an argon plasma at temperatures from 22,000K to 25,000K. A decrease in conductivity of this plasma could account for the decrease in δ_ϵ , but the existence of temperatures on the order of 22,000K is ruled unlikely, although a temperature profile at this power level was not attempted. The decrease in Q_c is possibly due to increased energy losses to the wall, since the highest temperatures occurred closer to the walls. Further work is needed to clarify the apparent contradictions that occurred during Mode 2 operation.

Inner tube diameter. The variations in plasma characteristics resulting from using a smaller diameter inner tube in Mode 3, show the effects of constricting the plasma, and thereby reducing the energy coupling and the effective radiation volume of the plasma, and the effect of the close approach to the wall by the plasma. The total effective coupling is low due to reduced energy coupling. The radiation characteristics are low due to the small radiation volume and probable lower plasma temperature, and the wall loss characteristics are high due to the close proximity of the plasma to the wall. The calorimeter characteristics are also noted to be high, but these values

are questionable. The possibility that the plasma extended down into the calorimeter during Mode 3 operation was previously mentioned. This event would result in measuring a certain amount of radial radiation in the calorimeter, and suggests that the values shown for the calorimeter characteristics are too high, and that the values shown for radiation characteristics accordingly are too low.

IV. Recommendations

General

The conclusions presented here were based on a study which just described the suffice of the research needed for the proper understanding of the behavior of the induction-coupled plasma. These conclusions represent the best that the present investigation has to offer.

The main areas for improvement and continued study brought out by this study are (1) the plasma-generator, (2) the coolant temperature measurement, (3) plasma temperature measurement, and (4) radiation power measurements.

An additional area for improvement through the use of the duty cycle control on the off-cooler supply should be studied. Duty cycles less than 100% will have an important benefit on the efficiency of a plasma-heated assembly when used as in the heater.

Plasma-Generator

The Injection Plate. The present gas injection plate with eight injection holes on a two-inch diameter circle offers no flexibility to gas injector, and the center of the plate is subjected to severe heating at high power operation. To add flexibility to gas injection, it is recommended that the injection system use two sets of injection holes drilled on different diameters. Each set of holes would be of different size and be supplied gas through independent gas manifolds.

This arrangement would allow the selection of different vortex strengths at the same total gas flow. In this manner, the effects of vortex strength could be shown. The results of this experiment could be reported as illustrated in Figure 18. The curves would be lines of constant gas flow. The leftmost point would represent 100% of the gas issuing from the manifold with the larger holes, and the rightmost point would represent 100% of the gas issuing from the manifold with the smaller holes.

A method for eliminating the heat loss on the injection plate was suggested by Dr. Soehnken. He suggested that a small amount of gas injected axially from the center of the injection plate would prevent the plasma from contacting the plate. As an extension of this idea, it might very well be possible to accurately position the top of the plasma by varying the axial gas injection which would control the reverse gas flow. Preventing the plasma from contacting the injection plate will allow operation at higher powers without contamination of the plasma by material from the injection plate.

Tube Diameters. The manner in which the power capability increases as the plasma extends suggests that the ratio of plasma diameter over rf coil diameter (D_p/D_c) is a parameter which should be studied. Studies should be made using larger diameter tubes, but keeping the same waterjacket thickness, or possibly reducing the waterjacket thickness, in order to increase D_p/D_c .

Plasma Heater. A large percentage of tube damage and breakage that occurred during this study could be directly attributed to "hot starts" with the vacuum start technique. Dr. B. B. Reed used an inductively heated plasma coil or refractory line loop to start the plasma current and pressure (Ref. 2; 21). The breakdown potential of the plasma heated by such a coil is not sufficient to allow ignition of the plasma by the coil itself. Starting the plasma at atmospheric pressure and then repeating the tube current experienced during vacuum startup, did not alleviate the need for a vacuum system. A result of this was the development of a higher coil or refractory line loop current. The coil is to be used with the device for starting purposes.

Coils. Several of the inner and outer tubes were provided by standard suppliers. Except for the section of the inner tube are subjected to severe heating, and cannot be reused. The outer tubes are heated by conduction and radiation through the Mylar tube. Should the plasma extend to the outer tube, it was started at 100% power, these button coils should hopefully still have the resistance required for an efficient heating. Some care, however, is required. If either temperature roughly 100° C. could be approached, that section of the outer coil cone rubber insulation, or in that case, the problem.

Water jacket. The space between the inner and outer tubes for a large part determines the water flow necessary to prevent local boiling next to the inner tube. Reducing this space, by proper selection of tube diameters, leads to smaller water flow requirements for the purpose of reducing local boiling. Reducing the water flow in turn reduces

the error in power measurements due to water temperature determination accuracy. If the waterjacket is made too thin, however, the black water technique for total power measurement may not be effective. In general though, smaller water flowrates, and higher temperature rises lead to better accuracies for power measurements, and therefore, a thin waterjacket should be considered.

Coolant Temperature Measurements

Coolant temperature measurements are very critical to power measurements, especially at high coolant flows. Temperature measurements accurate to the nearest one-half degree Fahrenheit would more nearly allow the magnitude of error in power measurements resulting from temperature inaccuracies to the magnitude of error resulting from water flow inaccuracies. Reducing temperature inaccuracies beyond this point will yield little in overall accuracy, and therefore become luxuries. At the least, temperature measurements should be accurate to the nearest degree Fahrenheit.

Plasma Temperature Measurements

An accurate knowledge of the temperature profile of an induction-coupled plasma is essential to the understanding of the basic phenomenon of induction-coupled plasmas, and to the development of theories to explain this phenomenon.

At present, W. G. Braun of the Physics branch, Aeronautical Research Laboratory, and C. Grabner, Chief of Analysis Branch, Digital Computation Division, aeronautical Systems Division, are developing a

computer program which will yield a spectral line intensity profile, $J(r)$, from an observed $N(x)$. The computer program will be applicable to any measurements for which axial symmetry can be assumed. When the program is established, the computer will fit an even ordered polynomial ($a_0 + a_2 x^2 + a_4 x^4 + \dots + a_{2n} x^{2n}$) to the observed data to obtain an analytical expression for $N(x)$. It will then differentiate $N(x)$ with respect to x , substitute $N'(x)$ into the integral equation, Eq (1), and perform the integration to obtain $J(r)$.

When this valuable tool is available to make multiple temperature profile determinations practical, a series of test runs in the pattern of this study should be made to determine the parameters which effect the maximum temperatures attainable, and the radius at which these maximum temperatures occur.

Radiation Power Measurements

Radiation power measurements in this study were hindered by two basic faults, other than inaccurate temperature measurements. The time difference between the clear water and black water readings is one fault, and the other fault is the inability to reproduce the plasma, as evidenced by the different values of I_e which occur at the same gas flow during the same data run. Ideally, all measurements are made simultaneously so that there is no time difference and no non-reproducibility problem.

Since plasma power is not time dependent while operating at a constant gas flow, measurements can be made at different times and still be valid if they do not depend upon reproducibility. This condition is satisfied by leaving the gas flow constant and switching the coolant supply between clear and black water to get measurements of both q_w and q_b . However, the black water used in this study deposited on the inner tube, and no clear water measurements could be taken after black water was once used. Therefore, an opaque coolant which does not deposit on the inner tube should be found for use in this radiation measurement technique.

A possible method for obtaining simultaneous power measurements was suggested by R. Winkerson, Physics Department, Air Force Institute of Technology. He proposed that the amount of radiation falling on a radiometer at some fixed distance from the plasma should be compared with the radiation measurements made by switching to black water without changing gas flow, to determine if the two radiation measurements are in some manner proportional. Using the present black water supply, this method entails cleaning the plasma-generator, between test runs. If a proportionality exists, then the radiometer should be carefully calibrated by a series of runs, so that subsequent radiation measurements can be made using the radiometer. The ability to obtain simultaneous power data is well worth the effort to calibrate the radiometer, therefore, tests for proportionality should be made.

Energy Balance

An energy balance on the plasma was not performed because no measurements of total electrical power transferred to the plasma could be made. There is a relatively simple method available to measure the electrical power absorbed by the plasma, but it requires additional instrumentation on the rf power supply. This method was suggested by Taylor and Hastings (Ref. 3; 1971). The additional instrumentation required is an rf ammeter in the circuit with the rf induction coil, and water flowmeters and thermocouples in the cooling system for the triodes in the rf power supply.

The total electrical energy supplied to the triodes can be measured with direct-current meters. The energy lost in the triodes is given off as heat and can be measured by reference to cooling water temperature rise and water flow. The energy not lost in the triodes is converted to rf energy output.

To obtain a measure of rf energy transferred to the plasma, the power supply is first operated in the absence of a plasma at some set value of rf current on the rf ammeter in the 'induction coil' circuit. Total electrical energy to the triodes and total triode losses are then measured as previously explained. The difference between these values is the rf energy losses which occur at that rf current. The power supply is next operated in the presence of a plasma, at the same rf current. The total triode energy input and losses are measured as before. The rf energy losses at this rf current were previously determined. The rf energy losses are added to the triode losses which

occurred on the second run, and this sum is then subtracted from the total energy supplied to the triodes on the second run. This difference is the energy which is transferred to the plasma.

By knowing the rf energy supplied to the plasma, a proper energy balance can be made. An energy balance is deemed necessary to validate the measurements made on the plasma by the techniques used in this study.

Supersonic Heating

The possibility of adding heat to the air in the supersonic region of a hypersonic wind tunnel by a rf induction-coupled plasma, was mentioned in the Introduction. However, plasma operation in gases with high linear velocities is unstable because the plasma cannot propagate fast enough upstream. In the vortex-stabilized plasma, ionized gas is blown upstream by the back-flow. This feedback system continuously supplies the ions necessary to maintain coupling between the rf induction coil and the plasma.

Stabilization by vortex flow in hypersonic wind tunnels cannot be considered, because it disrupts the gas flow. A schematic presentation of a stabilization scheme is shown in Figure 19. This scheme envisions a constant supply of electrons being injected into the gas flow near the throat of the wind tunnel. These electrons are carried downstream, by the fast moving gases, into the plasma coupling area where they couple with the rf induction coil, and thereby stabilize the plasma. As the electrons move downstream past the plasma area they are returned to ground, leaving a neutral gas behind.

The electrons can be generated in a typical electrodynamic ion-production method. For negative ion production, the corona discharge needle is given a high negative charge, just short of breakdown potential. The positive ions created near the needle point are attracted to the needle, whereas the negative ions are attracted to the nearby ground. Before the electrons can reach ground, however, they are carried downstream through the plasma-discharged area by the ion stream.

This stabilization scheme seems feasible. There is no doubt that the negative-ion stream can be generated; but only experimentation will show if this ion stream will couple with the induction coil, and if the current thereby generated will be sufficient to a volume small enough to prevent destruction of the tunnel walls. If coupling occurs without damage to the tunnel walls, the usefulness of this heat addition method is limited only to the extent to which the plasma experiences a heating effect caused by interaction between induction currents in the plasma and the field of the rf coil.

This heat addition system in the supersonic flow section of a hypersonic wind tunnel appears feasible, and should be checked by experimental means.

Duty Cycle as a Parameter

A duty cycle control on the rf power supply allows selection of any duty cycle desired between 0% and 100%. For any particular plate voltage setting, this allows selection of any plate power from zero to the maximum attainable on that plate voltage setting. Consequently,

with a prior knowledge of 'tuning plate power, P_0 , for that plate voltage setting, a particular value of P_0 can be selected exactly by use of the duty cycle control.

When the rf power supply is operated at a duty cycle less than 100%, the rf power is emitted in pulses at the rate of 300 per second. The duty cycle percentage corresponds to the length of those pulses. A duty cycle of 25%, for example, yields power pulses whose duration are 0.01 second, and when emitted at a rate of 300 per second, 0.025 seconds. Then, the rf power is emitted for 0.3 seconds.

Now, that a picture of this power supply is still conceivable, we important implications to the use of an inductively coupled plasma as a source, such as heating, pumping and ionizing. One of the characteristics of plasma, such as found in an arc-discharge arc, is that they are so violent they defy efforts to blockade current in the arc channel. After a time, the effectiveness of heating insures by electric arcs. The short contact of arcs can be circumvented in a pulsed induction-coupled plasma, because the heat of resistive ion heating the cold gases by moving them through the plasma, the plasma moves to through the cold gases. High speed photographs taken of a plasma operating at a duty cycle of 50, clearly show the pulsating nature of the plasma. When the power pulse ends the plasma rapidly collapses, and the radiating plasma gradually shrinks toward the center of the tube. When the next power pulse occurs, it couples with the remaining conducting gas, and the plasma gradually swells to normal size. The pulsing of the plasma is not visible to the eye, and normal size refers

to the size of the plasma seen by the eye. It is proposed that this pulsing action of the plasma more effectively heats the gas than operation of the plasma at a duty cycle of 100%, because wall losses and radiation should decrease due to pulsing the power. A series of tests would be run at the same gas flow and P_0 on the nine possible plate voltage settings to confirm or deny this proposal.

Summary

Very little information is available on induction-coupled plasmas to date. This study is the only work known to the author which is available on induction-coupled plasma operation below the megacycle range. The information is by no means detailed enough to tax the ingenuity of the investigator to use it. It is probable that sufficient information is available to investigate plasmas in pure gases other than argon if plasma energy, if a plasma-generator is developed to contain it, is available. When so conducted on induction-coupled plasmas are no longer used, it would be desirable to utilize a sustained, long-term source of investigation. This study has established the general characteristics of a high-power induction-coupled plasma-generator, and has revealed a number of experimental difficulties which must be considered. Thus a comprehensive program of investigation may now be confidently undertaken.

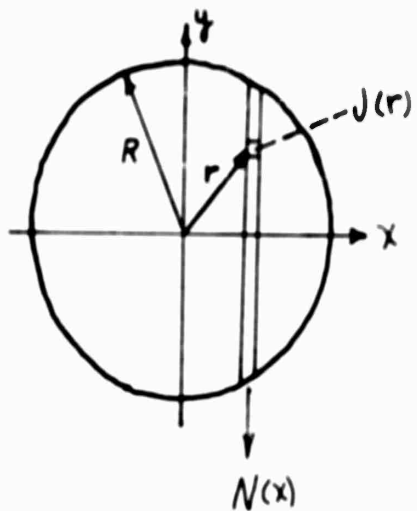
Bibliography

1. Olsen, H. N. "Thermal and Electrical Properties of an Argon Plasma". The Physics of Fluids, 2:614-623 (1959).
2. Reed, Thomas B. "Induction-Coupled Plasma Torch". Journal of Applied Physics, 32:821-824 (1961).
3. Taylor, A. Hoyt, and H. F. Hastings. "The Determination of Power in the Antenna at High Frequencies". Proceedings of the Inst'tute of Radio Engineers, 19:1370-1373 (1931).

Appendix A

Abel's Integral Transformation

The transversely observed rad'ence of the plasma 'image', $N(x)$, is inverted to the radiant intensity, $J(r)$, in the following manner.



$$N(x) = 2 \int_0^y J(r) dy$$

But,

$$y = \sqrt{r^2 - x^2}$$

And,

$$dy = \frac{r dr}{\sqrt{r^2 - x^2}}$$

Therefore:

$$N(x) = 2 \int_x^R \frac{J(r) r dr}{\sqrt{r^2 - x^2}}$$

This is Abel's integral, which inverts analytically to form

$$J(r) = -\frac{1}{\pi} \int_r^R \frac{N'(x) dx}{\sqrt{x^2 - r^2}}$$

The prime 'indicates differentiation with respect to x.

Figuras

GA/Phys/62-2

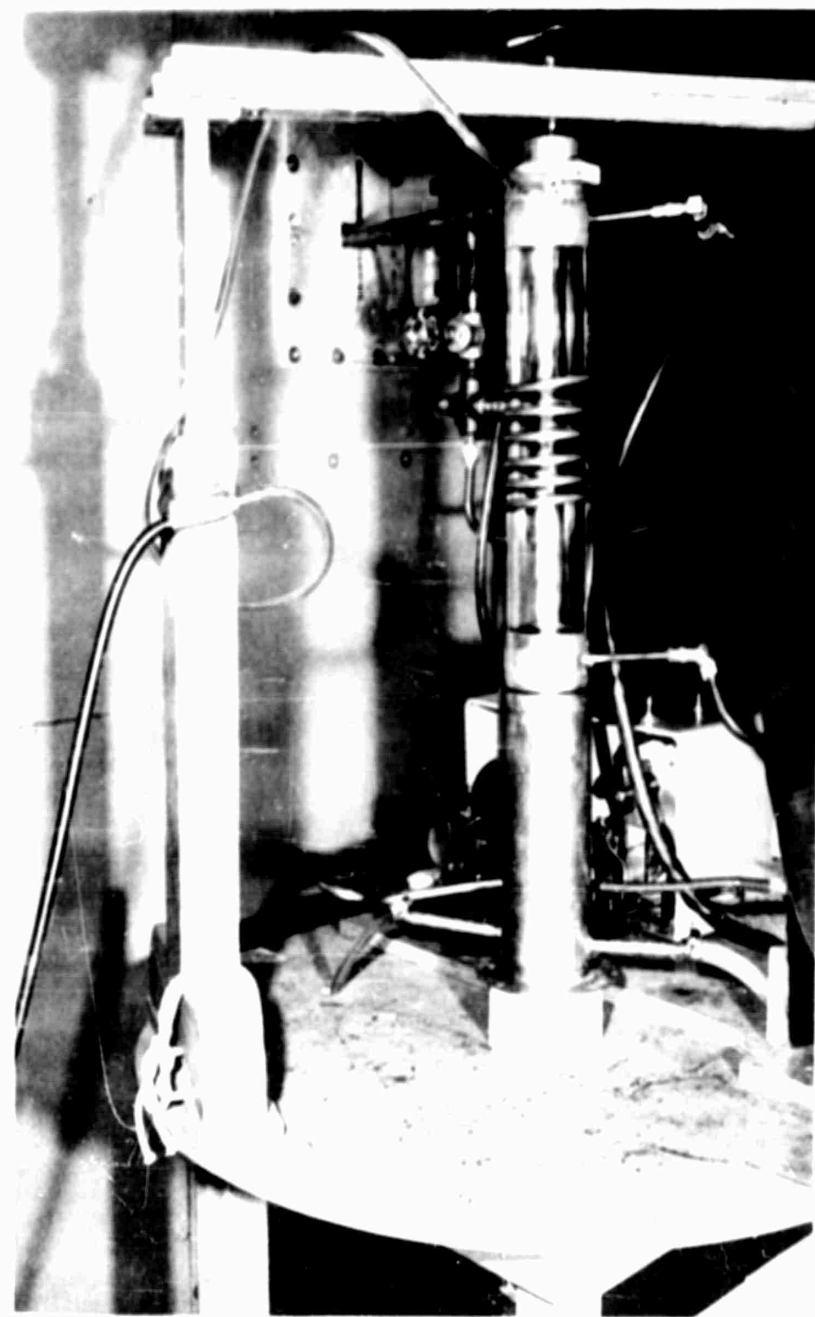


Fig. 1
Plasma-generator with
clear water coolant

GA/Phys/62-2

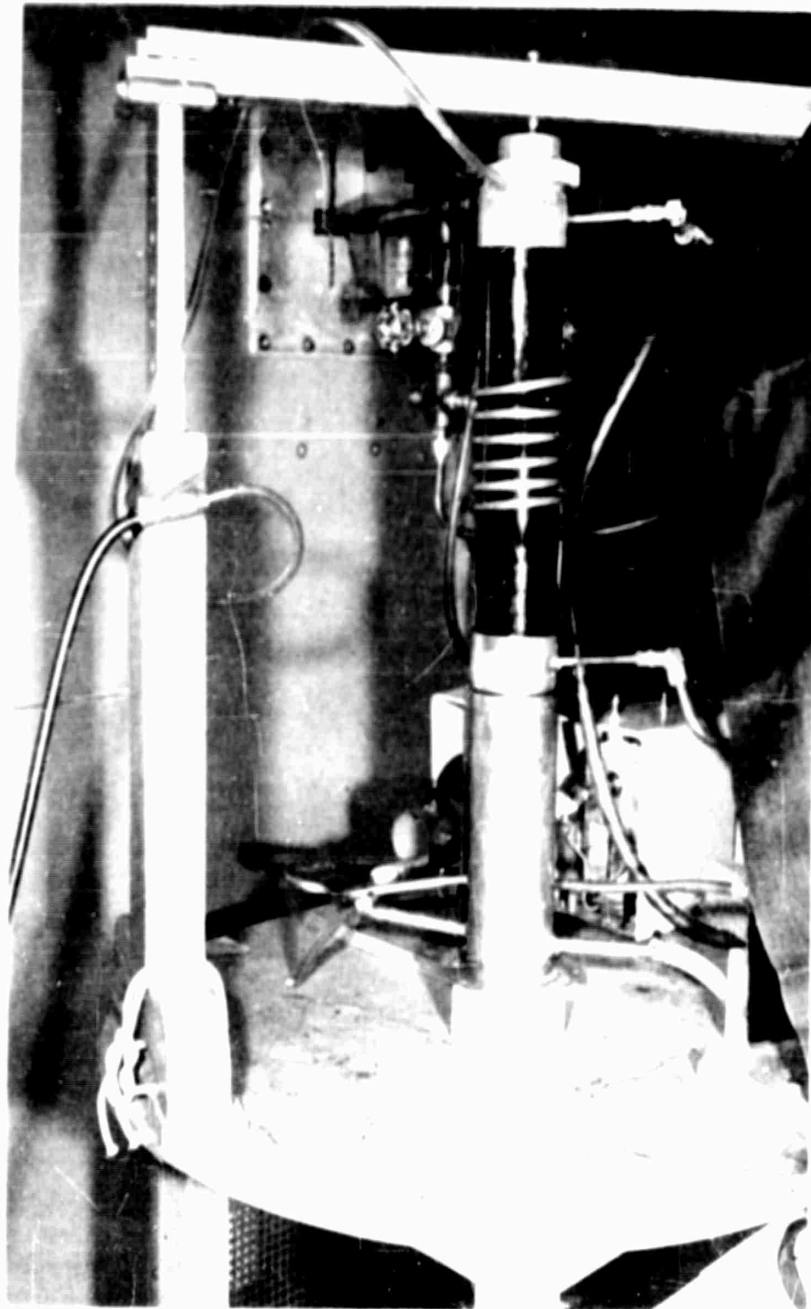


Fig. 2
Plasma-generator with
black water coolant

GA/Phys/62-2

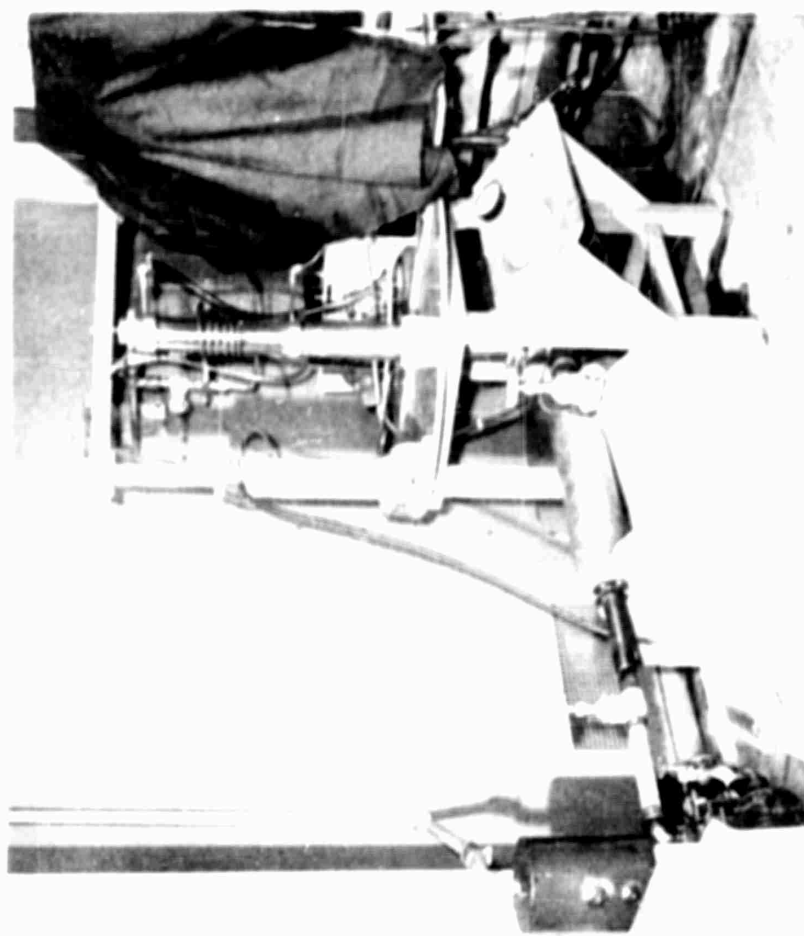


Fig. 3
Experimental apparatus

GA/Phys/62-2

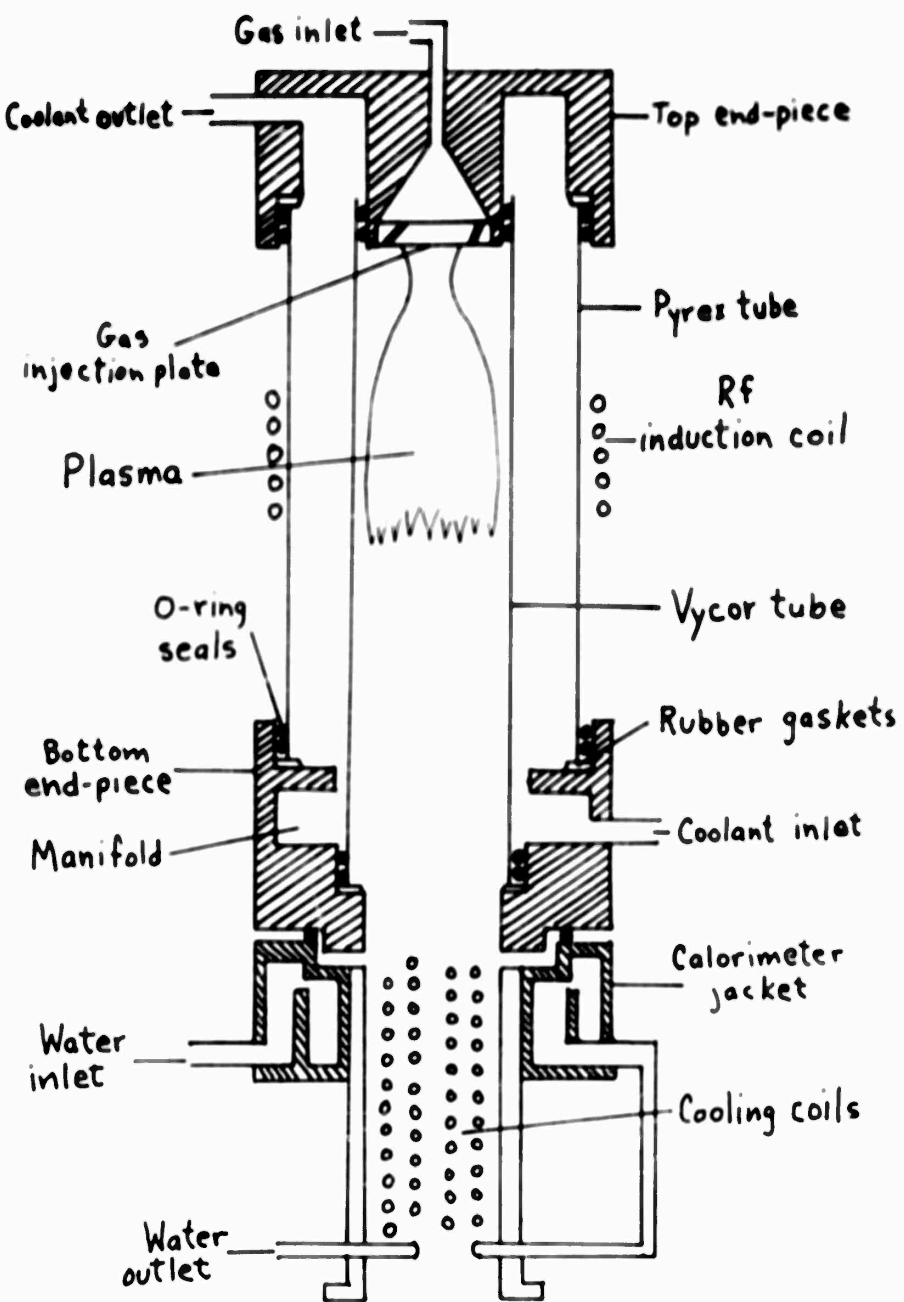
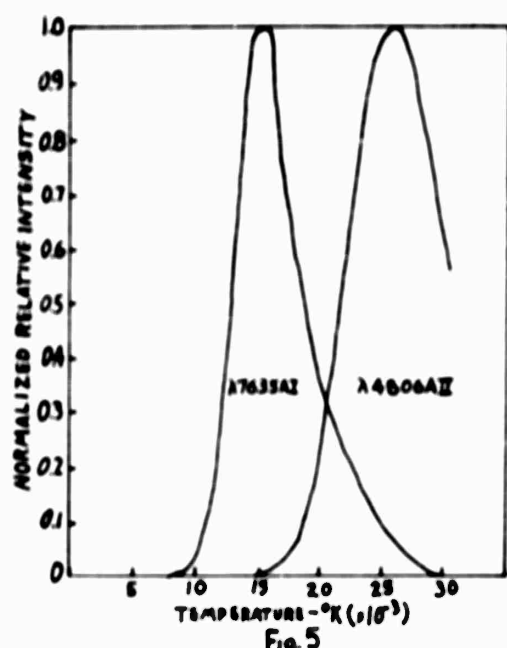
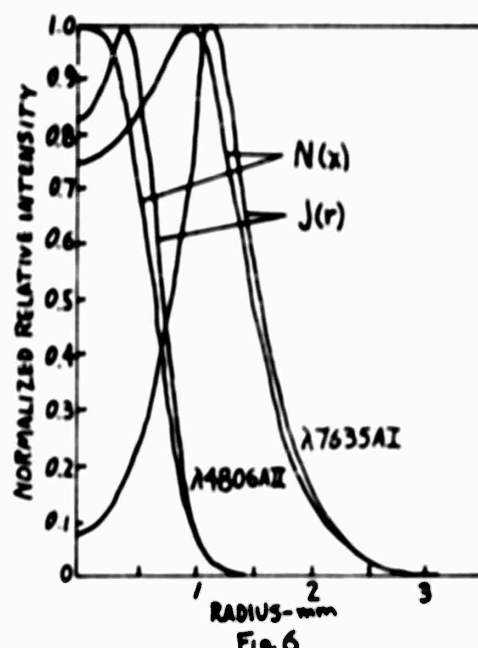


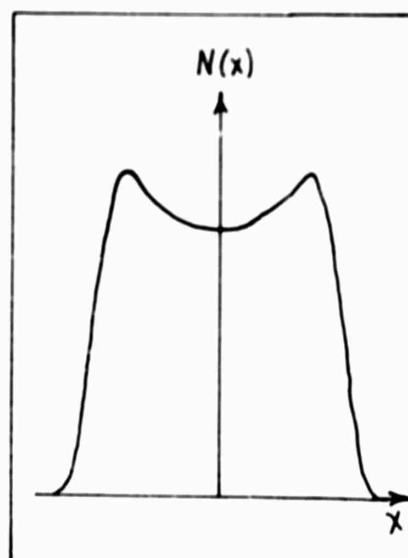
Fig. 4
Schematic of plasma-generator and calorimeter



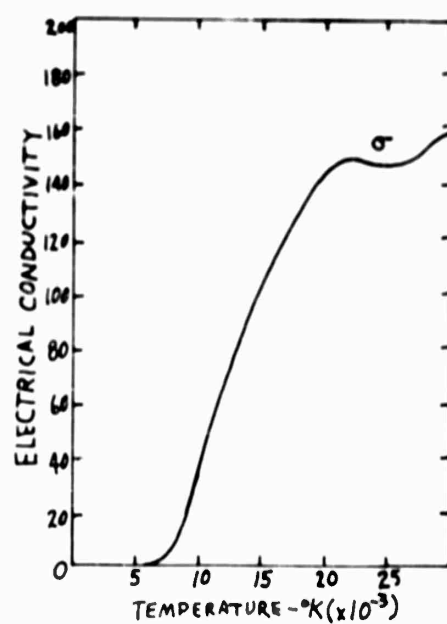
(From Ref 1:617)



(From Ref 1:616)



Typical observed intensity
of λ7635AI



(From Ref 1:620)

GA/Phys/62-2



Fig. 9
Modified outer tube
for Mode 3

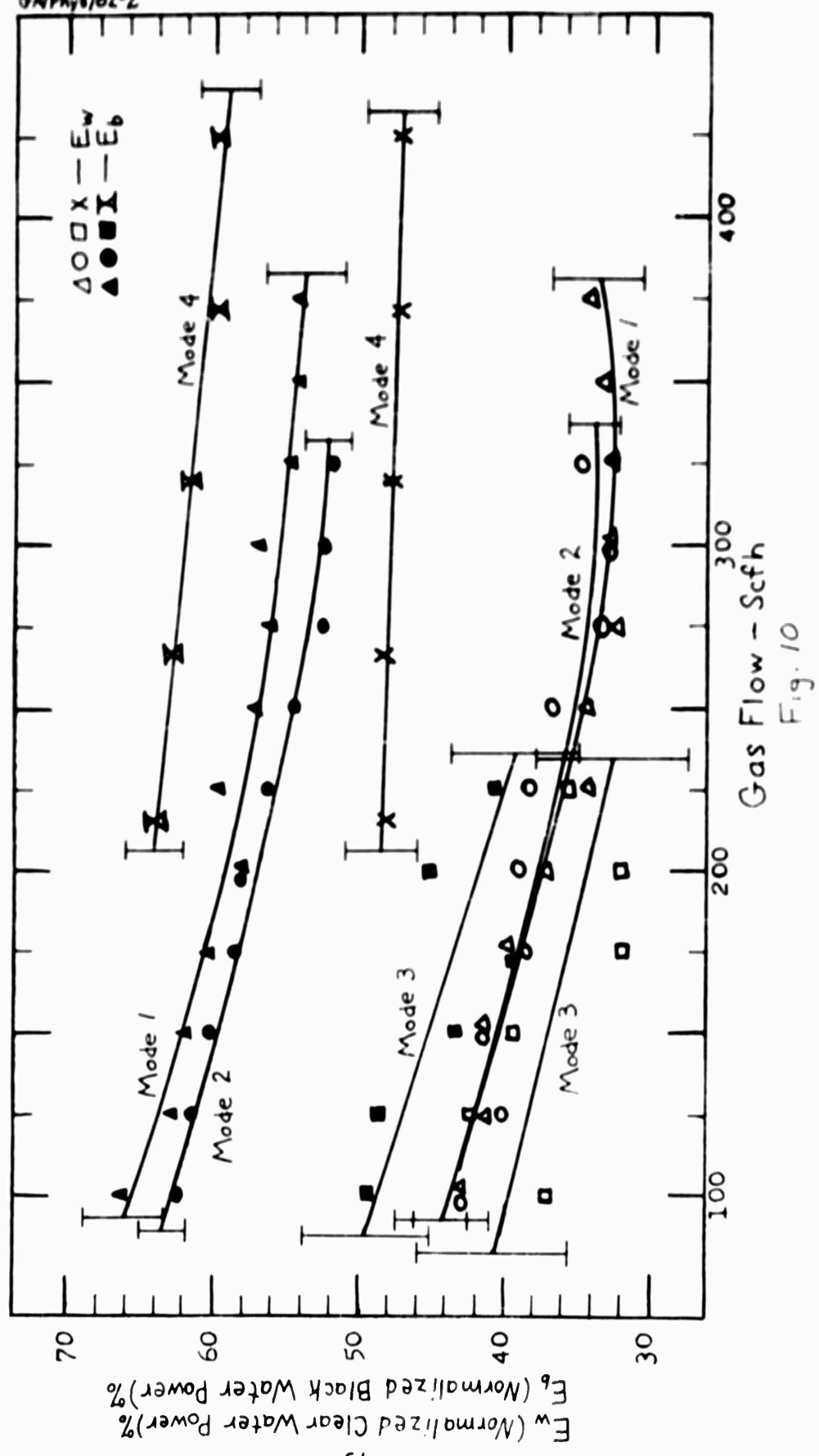


Fig. 10

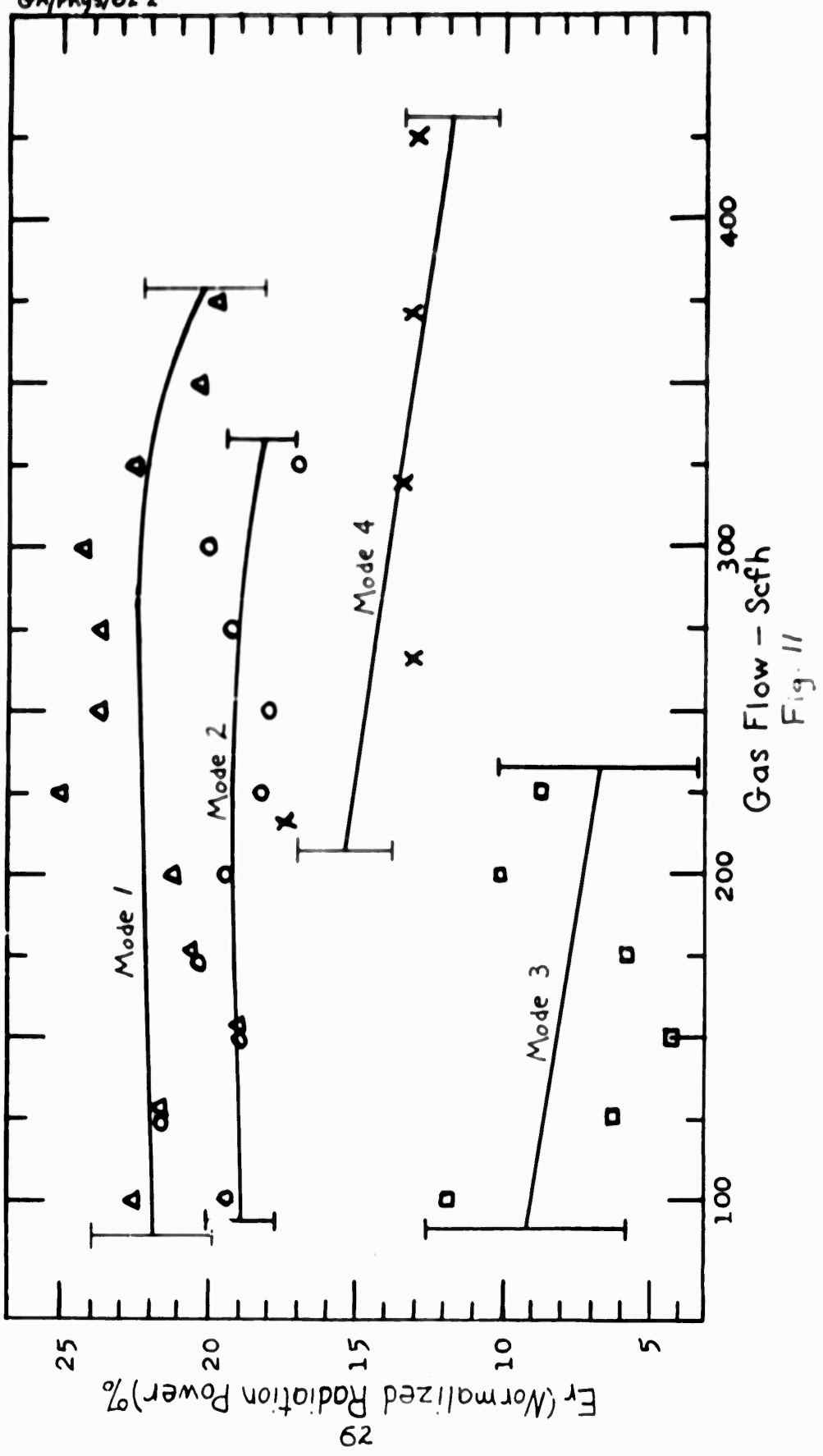
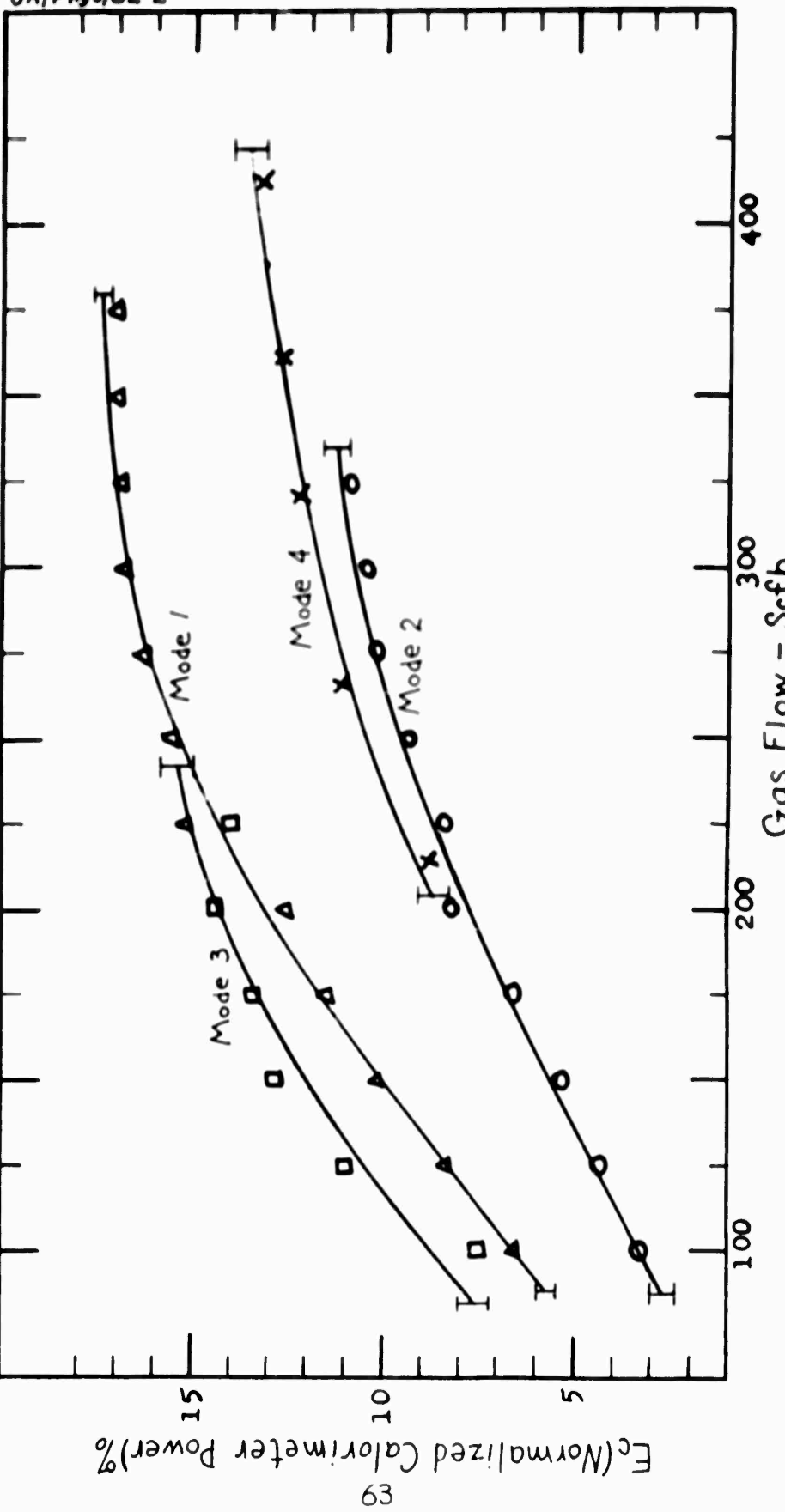
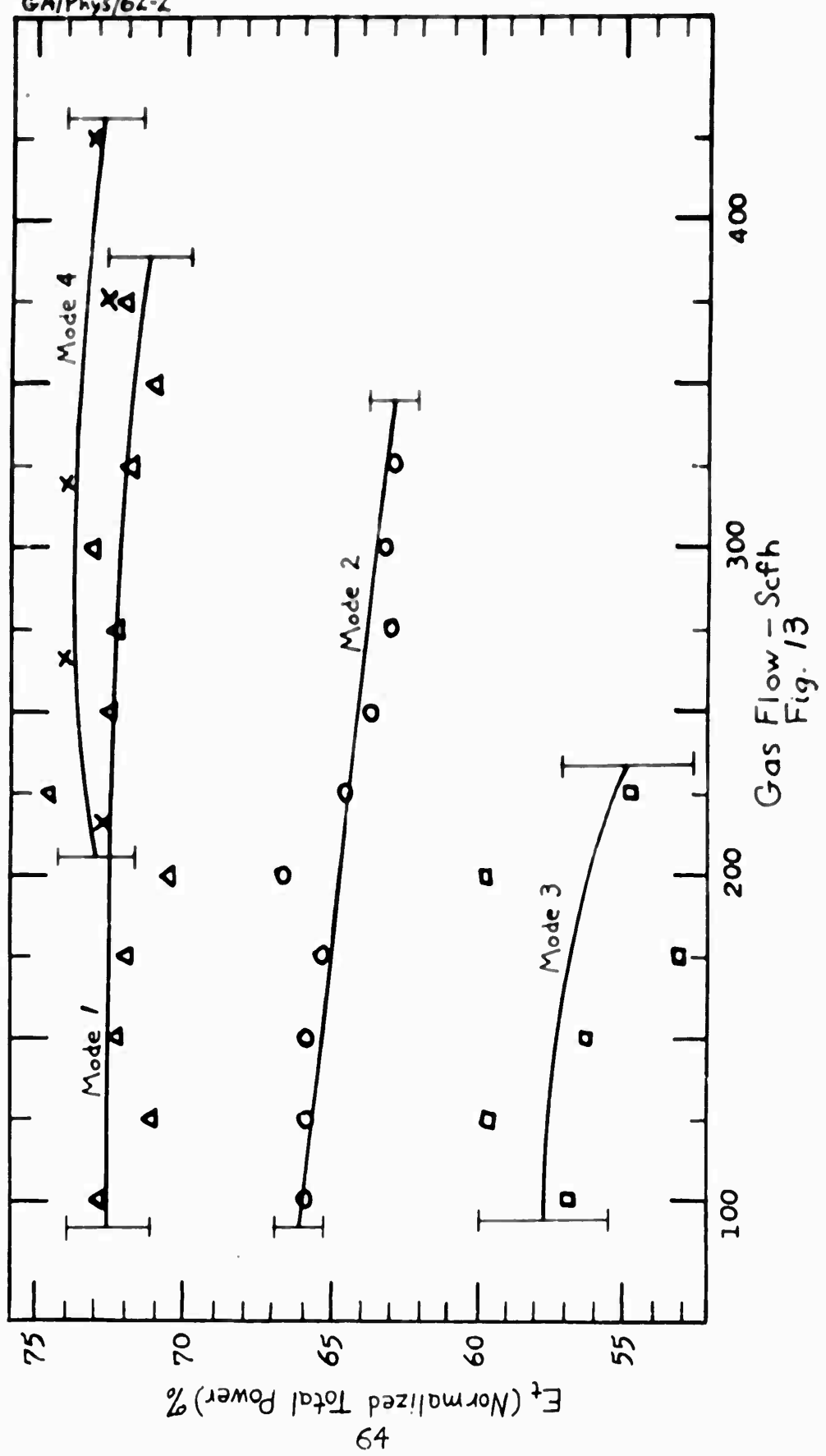


Fig. 11



Gas Flow - Scfh
Fig. 13

GA/Phys/62-2

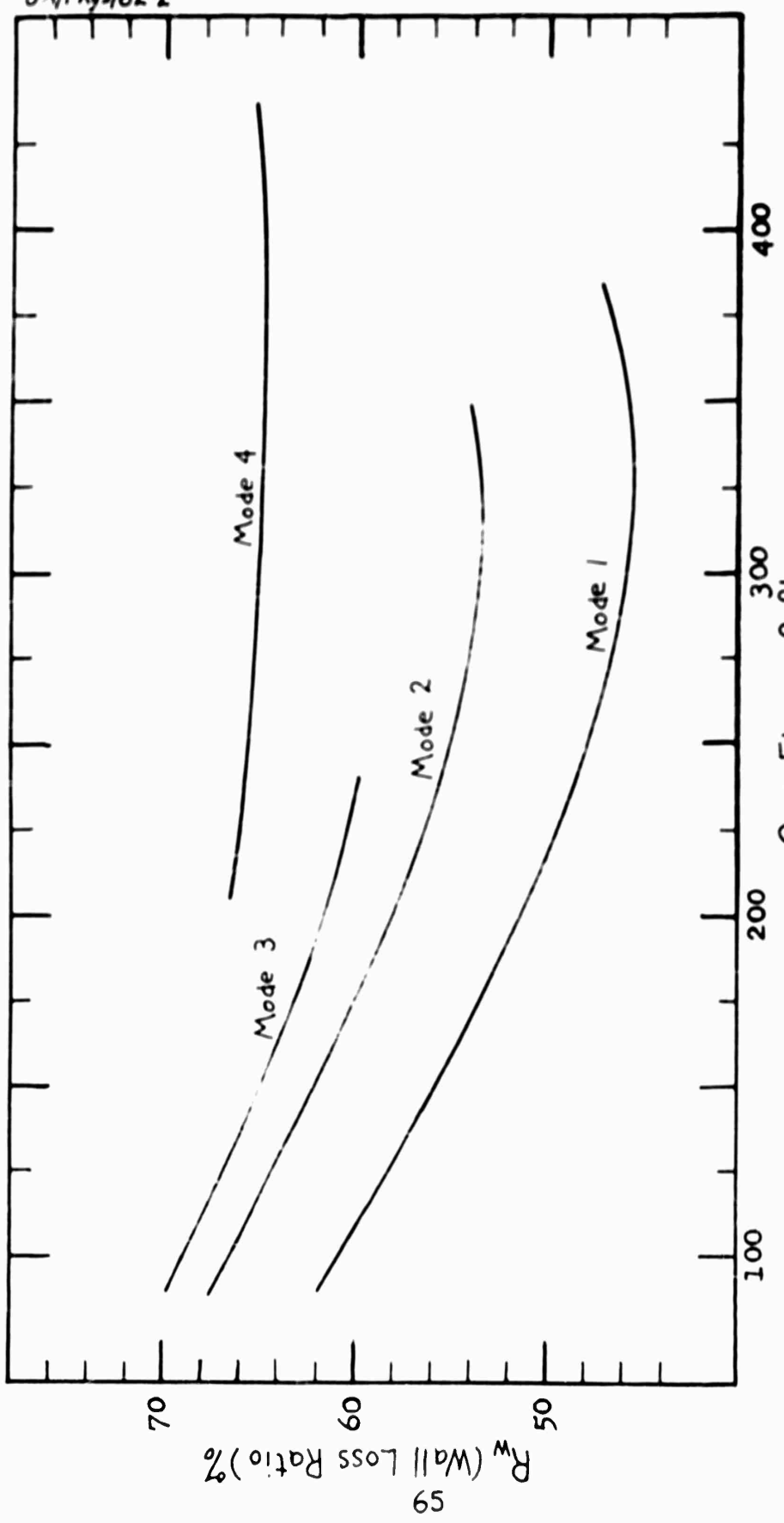


Fig. 14

GA/Phys/62-2

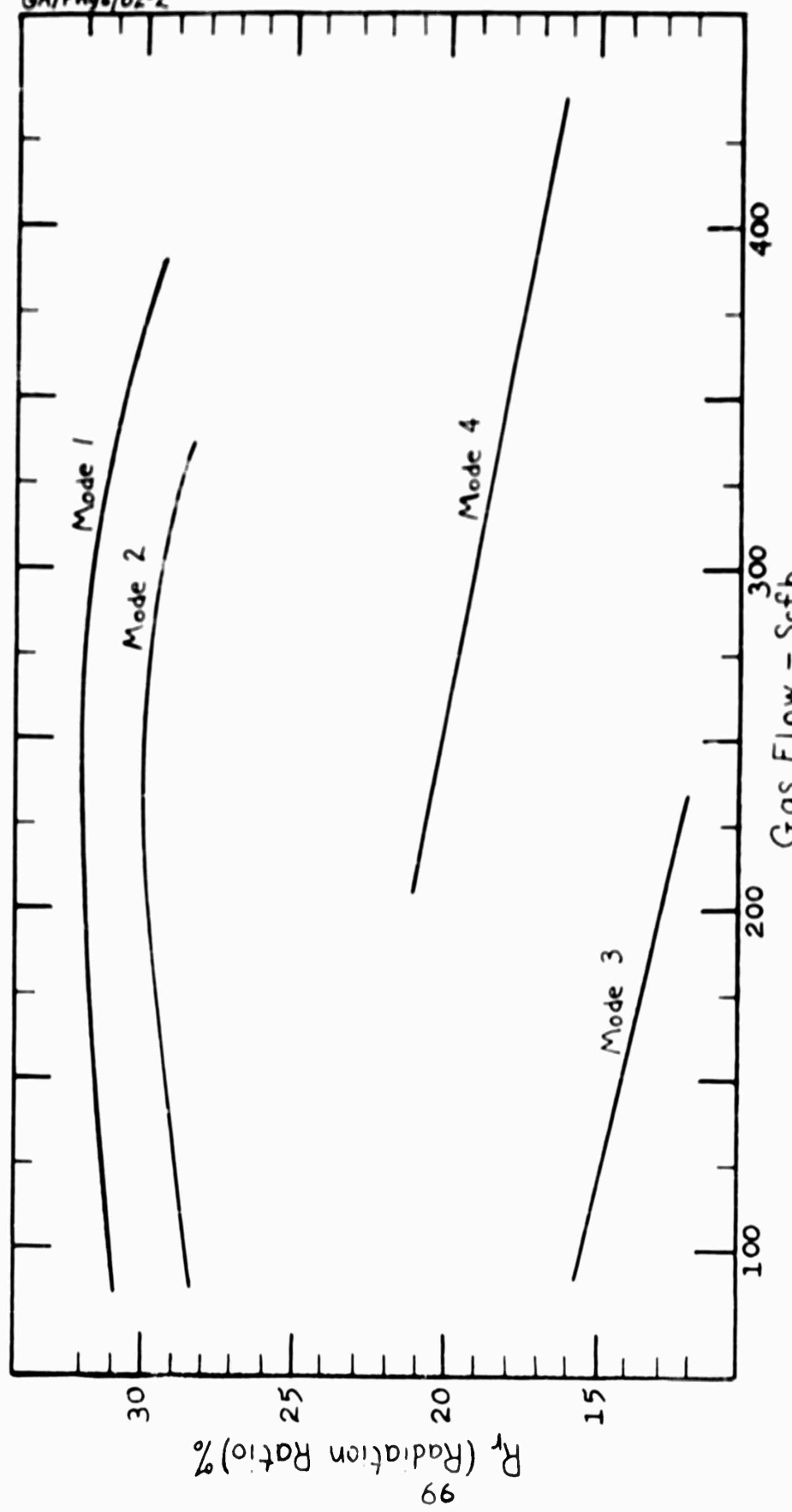


Fig 15

GA/Phys/62-2

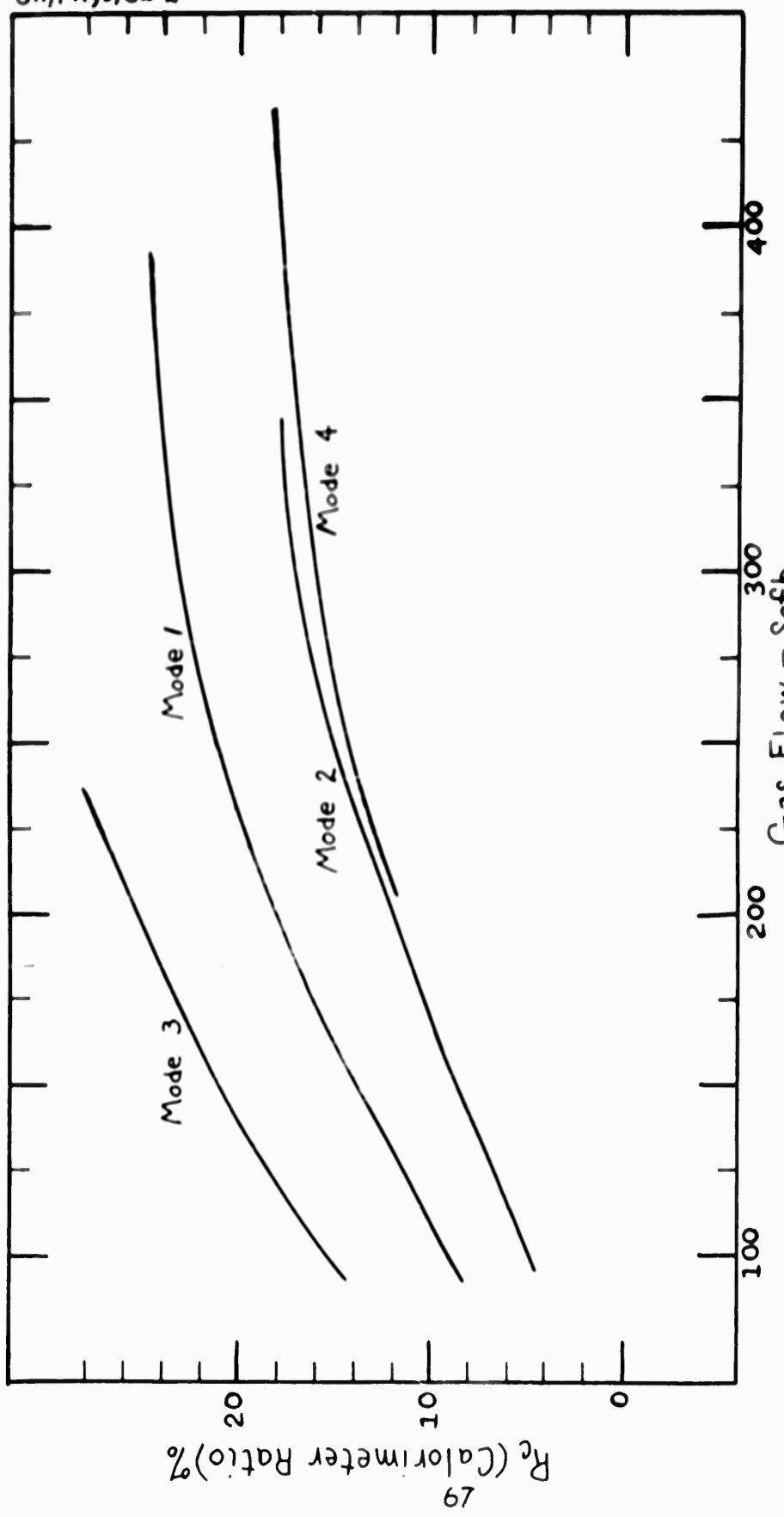
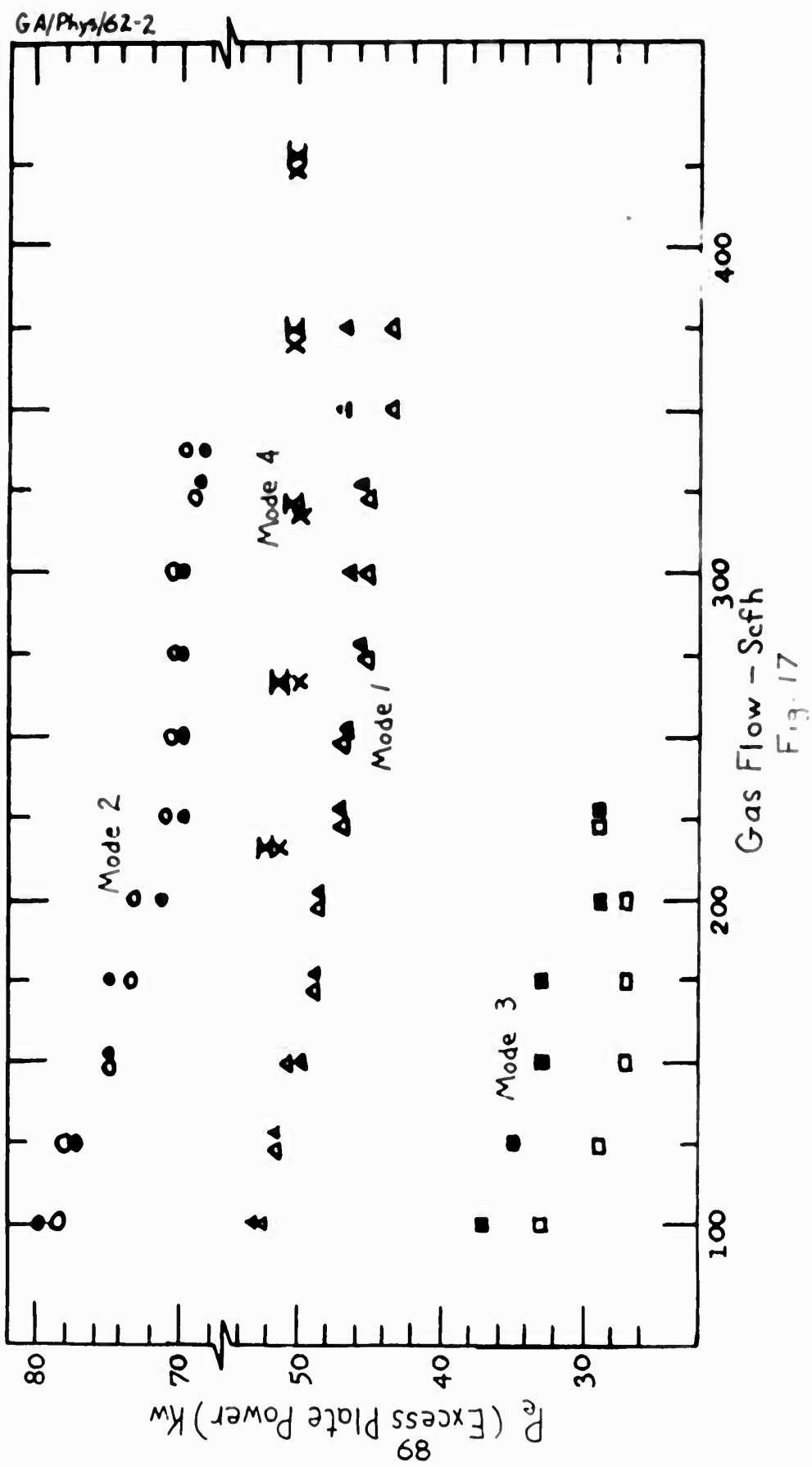


Fig. 16



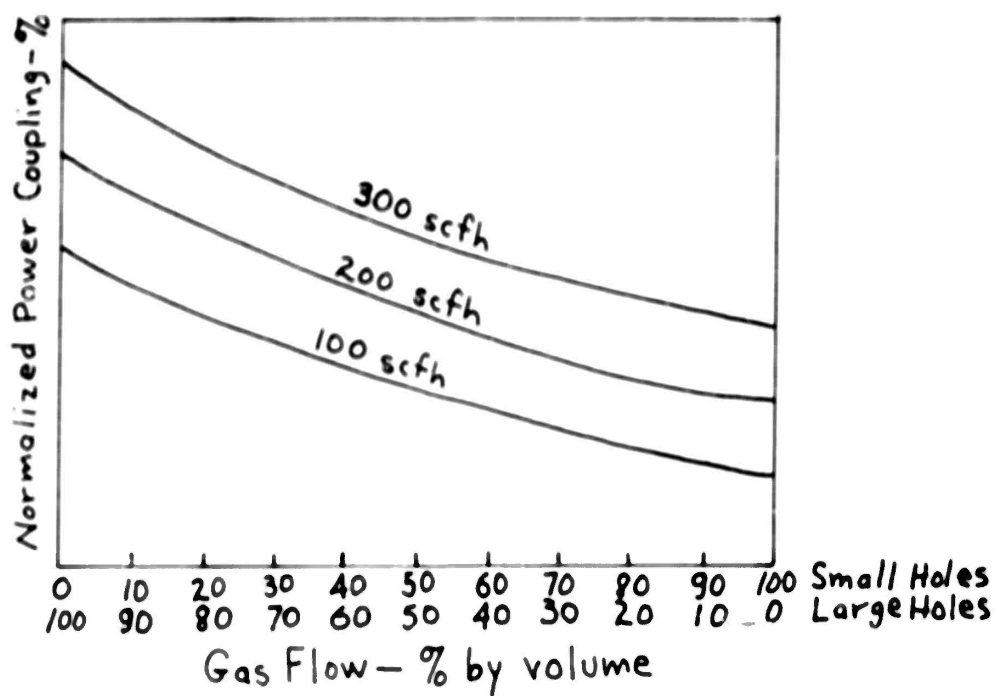
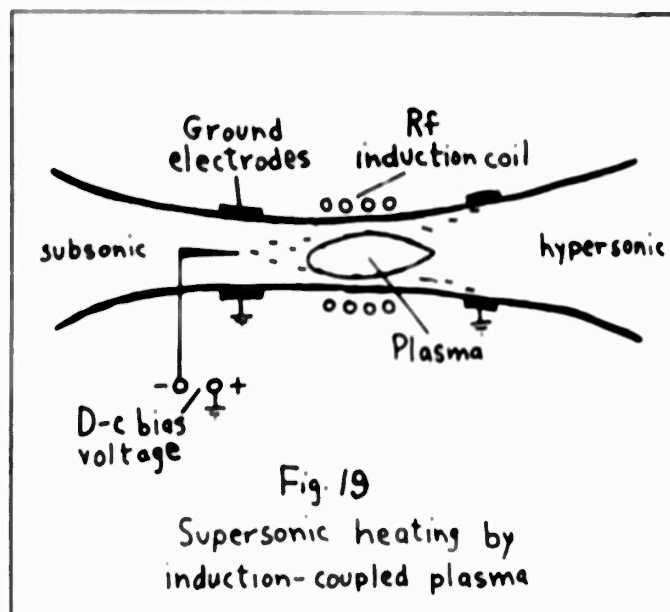


Fig. 18

Power coupling as a function
of changing vortex strength,
with excess plate power and
total gas flow constant



Vita

Howard R. Cannon was born on [REDACTED]

[PII Redacted]

He graduated from northeast high school in Denver City, Colorado in 1947. In 1951, he enlisted in the United States Air Force, and was appointed to the United States Military Academy from the regular Air Force. In June 1955, on 3 June 1956, he was commissioned a Second Lieutenant in the regular Air Force, and he graduated from the United States Military Academy on 5 June 1956 with a Bachelor of Science degree in Military Science. Prior to admission to the Air Force Institute of Technology, he served as a combat operations officer in Korea, Korea.

Ensign [REDACTED] [REDACTED] [REDACTED] [REDACTED]
[REDACTED] [REDACTED] [REDACTED] [REDACTED] [REDACTED]

[PII Redacted]

Ensign [REDACTED] [REDACTED] [REDACTED] [REDACTED]

[PII Redacted]